STRESS ANALYSIS OF AN ELLIPSOIDAL INCLUSION

by

Mahesh Kailas

Presented to the Faculty of the Graduate School of

The University of Texas at Arlington in Partial Fulfillment

of the Requirements

for the Degree of

MASTER OF SCIENCE IN MECHANICAL ENGINEERING

THE UNIVERSITY OF TEXAS AT ARLINGTON

AUGUST 2007

ACKNOWLEDGEMENTS

I would like to take this opportunity to thank my supervising professor Dr. Seiichi Nomura for his invaluable advice, encouragement and motivation. I am thankful to Dr. Wen Chan and Dr. Dereje Agonafer for agreeing to serve in my thesis advising committee and for their guidance thought my Masters program. I would like to thank all professors from the Department of Mechanical Engineering, The University of Texas at Arlington for their valuable guidance throughout course of my masters.

I am thankful to all my friends for their support and encouragement. I like to thank all my family members and relatives for their support. Finally, I like to thank my parents for their invaluable support, motivation and guidance. I am grateful for their persistence in channeling my academic goals and ambitions.

July 20, 2007

ABSTRACT

STRESS ANALYSIS OF AN ELLIPSOIDAL INCLUSION

Publication No. _____

Mahesh Kailas, M.S.

The University of Texas at Arlington, 2007

Supervising Professor: Dr. Seiichi Nomura

The focus of the present thesis is to develop a mathematical model to calculate the stresses inside an ellipsoidal inclusion present in an infinitely extended matrix region and to validate the mathematically derived model by the Finite Element Method. To this end, a theoretical model has been developed to predict the stress inside an ellipsoidal inclusion. This model is based on equivalent inclusion method used to evaluate the stress distribution theoretically. Though there have been many theories to predict the stress distribution inside an ellipsoidal inclusion, its numerical validation is new despite its importance. A finite element model of a matrix-inclusion pair has been employed based on continuum mechanics approach. The interface surface between the matrix and the inclusion is modeled using suitable a contact element.

The finite element analysis was carried out by assigning different properties for the matrix and inclusion region. Analysis with varying aspect ratio and elastic moduli of the inclusion region was also carried out to study the influence of the size and material property on the stress inside the inclusion. The finite element method shows that the stress distribution inside the inclusion is almost constant as predicted by the theoretical model. The above analysis also validates the use of the finite element method based on the continuum mechanics approach in studying the overall behavior of the inclusion problems.

TABLE OF CONTENTS

ACKNOWLEDGEMENTS iii

ABSTRACT iv

LIST OF ILLUSTRATIONS ix

LIST OF TABLES xi

Chapter

1. INTRODUCTION 1

1.1 Introduction to composite materials. 1

1.2 Inclusion Problem 3

2. EQUIVALENT INCLUSION METHOD AND ESHELBY'S TENSOR. 7

2.1 Introduction 7

2.2 Equivalent Inclusion Method 8

2.3 Eshelby's Tensor 10

3. FINITE ELEMENT MODELING OF MATRIX AND INCLUSION 11

3.1 Introduction 11

3.2 Modeling steps of matrix and inclusion 11

3.2.1 Finite Element Modeling 11

3.2.2 Assigning Material Properties 13

3.2.3 Defining the Contact Element……...…… 14

3.2.4 Meshing 15

3.2.5 Mesh Refinement of the Inclusion ……..... 15

3.2.6 Applying Loads and Displacements..... 16

4. MATHEMATICAL AND FINITE ELEMENT MODELING OF ELLIPSOIDAL INCLUSION...…..... 18

4.1Introduction..... 18

4.2 Mathematical Modeling……..... 18

4.3 Shear Stress Validation for a Spherical Inclusion. ……. 20

4.3.1 Mathematical Model……..... 20

4.3.2 Finite Element Model of the Spherical Inclusion..... 22

4.3.3 Ansys Post Processing 23

4.4 Shear Stress Validation for Spherical Inclusion along the 12 Direction 26

4.4.1 Finite Element Model of the Ellipsoidal inclusion..... 29

4.4.2 Ansys Post Processing 30

4.5 Shear Stress Validation for Spherical Inclusion along the 23 Direction 34

4.5.1 Ansys Post Processing 35

4.6 Normal stress validation for an ellipsoidal inclusion 37

4.6.1 Finite Element Model 43

4.6.2 Ansys Post Processing …….. 44

5. CONCLUSIONS AND FUTURE SCOPE OF WORK …….. 52

5.1 Conclusion …… 52

5.2 Future Scope of Work ……52

REFERENCES..... 54

BIOGRAPHICAL INFORMATION 55

LIST OF ILLUSTRATIONS

Figure Page

1.1 Aluimino Silicate Platelets in polyamide-6 matrix 3

1.2 Matrix D and Inclusion Ω 4

2.1 Inclusion C^i in a matrix C^m 8

2.2 Ellipsoidal Inclusion with semi principle axes a_1, a_2, a_3 10

3.1 3-D CAD model of the matrix and inclusion (solid model) 13

3.2 Bonded contact region of the inclusion 14

3.3 Meshed matrix and inclusion region 15

3.4 Finer mesh refined inclusion region..... 16

3.5 Loading and displacements on the matrix region 17

4.1 FEA model of the matrix -spherical inclusion 23

4.2 Strain plot of the spherical inclusion analysis 24

4.3 Stress plot of the spherical inclusion 25

4.4 The Ellipsoidal Inclusion 29

4.5 FEA model of the matrix and ellipsoidal inclusion..... 30

4.6 The strain plot of the matrix and ellipsoidal inclusion 31

4.7 Stress plot of the inclusion region 32

4.8 The stress plot in 23 directions..... 35

4.9 FEM model of matrix and inclusion.....44

4.10 The strain plot in 11 direction……. 45

4.11 The strain plot in 22 direction 46

4.12 The strain plot in 33 direction 46

4.13 The stress plot in 11 direction 47

4.14 The stress plot in 22 direction 48

4.15 The stress plot in 33 direction 48

LIST OF TABLES

Table Page

3.1 Material Property of the Matrix and Inclusion 13

4.1 Material Property of the Matrix and Inclusion 19

4.2 Shear Stress Validation for different ratio Matrix –Inclusion E values..... .. 26

4.3 The Stress, Strain and S values for different aspect ratios. (12 components)..... 33

4.4 The stress, strain and S values for different aspect ratios (23 components) 36

4.5 I values –Normal component 40

4.6 S values–Normal component 41

4.7 Elastic Modulus of Normal components for Matrix 42

4.8 Elastic Modulus of Normal components for Inclusion 42

4.9 Comparison between the ansys and theoretical values..... 49

4.10 Stress, Strain and S values (Normal components)..... 50

CHAPTER 1

INTRODUCTION

1.1 Introduction to composite materials

With our continuing quest for lighter and stronger composites, the demand for new types of composite materials is increasing. In recent years various composite materials have been used extensively in aircraft structures, space vehicles, automobiles, sporting goods, electronic packaging to medical equipment, and many consumer products. The main advantage of composite materials is the potential for a high ratio of stiffness to weight, corrosion resistance, high fatigue strength etc…

A composite material consists of one or more bonded discontinuous phases distributed in one continuous phase. The discontinuous phase which is also called as the reinforcement phase or fillers has enhanced material properties than the continuous phase called as matrix. The properties of a composite material are a result of material properties of constituent materials, their geometric distribution and their interactions. The concentration of the reinforcement is usually measured by the volume fraction or by the weight fraction. The concentration of the reinforcement is a determining parameter of the properties of the composite material. For a given concentration, the distribution of the reinforcement in the volume of the composite is also an important parameter. A uniform distribution will ensure "homogeneity" of the material *i.e.* the properties of composites are broadly classified as fibrous composites and particles

composites. If the reinforcement is in the form of fibers, the composite material is called as a fibrous composite. The fibers used may be continuous, discontinuous, chopped fibers, short fibers, etc Particulate composites are made of particle reinforcement materials. Particles are generally used to improve certain properties of the materials such as stiffness, behavior with temperature, resistance to abrasion, decrease of shrinkage, etc. Composites are also classified based on the nature of the constituents as organic matrix composites, metallic matrix composites and mineral matrix composites (ceramic). The most common advanced composites are polymer matrix composites (PMCs) consisting of a polymer reinforced by fibers. The most common fibers used are glass, carbon, Kevlar, silicon carbide (SiC), boron, aluminum etc…

For efficient design and formulation of composites, it is important to have appropriate theories for the prediction of mechanical properties, thermal expansion, and other behavior in terms of the elastic properties of the matrix and filler, the geometry of the filler particles (or inclusions), and the overall morphology of the composite. The various theories for composites usually regard the filler particles as spherical, cylindrical, or disc shaped .More so most inclusion shapes can be approximated by some ellipsoidal

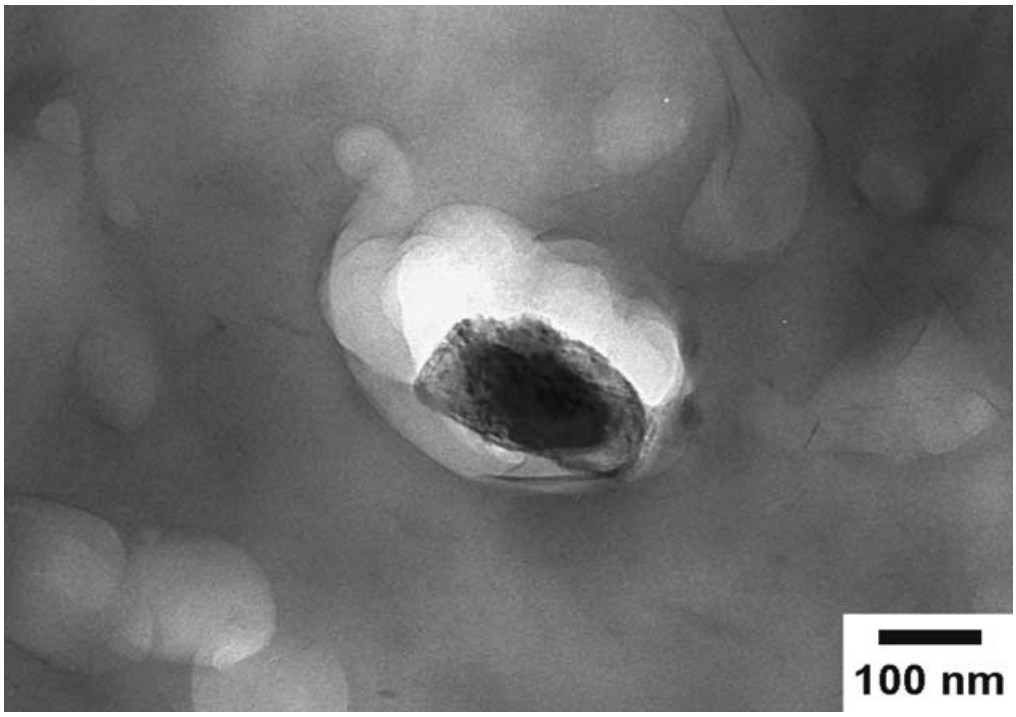

Fig 1.1 Aluimino Silicate Platelets in polyamide-6 matrix [3]

1.2 Inclusion Problem

One of the most challenging parts of composite materials in micromechanics is an inclusion problem.. Consider a region D in which a part Ω has its temperature raised by delta T, the thermal stress

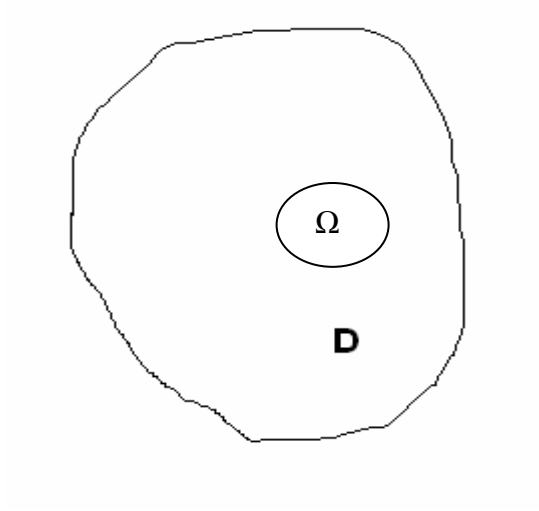

Fig 1.2 Matrix D and Inclusion Ω

σ_{ij} is induced in the material D by the constraint from the part which surrounds Ω.The thermal expansion is αT where α is a linear thermal expansion coefficient . The thermal strain is expressed as

$$\varepsilon_{ij}^{*} = \delta_{ij}\,\alpha\,T \qquad (1.1)$$

where δ_{ij} is the Kronecker delta. The thermal expansion strain is the strain caused when Ω can be expanded freely with the removal of constrain from the surrounding part. The actual strain is then the sum of the thermal and elastic strains. The elastic strain is related to the thermal stress by the Hook's law. The thermal expansion strain is a typical example of an eigenstrain. In the elastic theory of eigenstrains and eigenstress, however it is not necessary to attribute ε_{ij}^{*} to any specific source. Although the above illustration was done in terms of thermal strain, the source could be phase transformation, precipitation, plastic deformation or a fictitious source necessary for the equivalent inclusion method.

When an eigenstrain ε_{ij}^{*} is prescribed in a finite subdomain Ω in a homogeneous material D and it is zero in the matrix D- Ω, then Ω is called an inclusion. The elastic moduli of the material are assumed to be homogeneous when the inclusions are under consideration.

If a sub domain Ω is a material D which has elastic modulus different from that of the matrix, then Ω is called an in homogeneity. Applied stresses will be disturbed by the existence of the in homogeneity. The disturbed stress field will be simulated by an eigenstress field by considering a fictitious eigenstrain ε_{ij}^{*} in the homogeneous material. When this region (the inclusion) in an infinite homogeneous isotropic elastic medium undergoes a change of shape and size which, but for the constraint imposed by its surroundings (the "matrix"), is an arbitrary homogeneous strain .What is elastic state of the inclusion and matrix?

The answer to the above question was first dealt by J D Eshelby in 1957 in his celebrated paper entitled 'The Determination of the Elastic Field of an Ellipsoidal Inclusion, and Related Problems ` [1]. Eshelby (1957, 1959, 1961) developed a simple and elegant method for the solution of the inclusion problem in isotropic solids. In this problem, an arbitrary part of an unbounded homogeneous isotropic medium is a misfit inclusion or an in homogeneity that would undergo an arbitrary infinitesimal uniform strain (stress free transformation strain, misfit strain or eigen strain), ε_{ij}^{*} if its surrounding material were absent. Unlike the usual approach of standard methods of applied mathematics, the solution for the homogeneous inclusion is obtained with the

help of a sequence of imaginary cutting, straining and welding operations, and the displacements are expressed in term of the volume integral (over the volume of the inclusion) of the product of the point force Green's function and the eigenstrain. The reasoning leading to the expression for the displacements due to a transformed inclusion of any shape in an isotropic solid applies equally to an anisotropic material [2]. Eshelby also pointed out that to obtain explicit expressions analogous to those for isotropic solids, one should have to know the form of the displacement due to a point force in an anisotropic solid. Eshelby [1] carried the analysis far enough to show that the stress is uniform inside a transformed anisotropic ellipsoid in an anisotropic matrix

The purpose of the present paper is validation of J D Eshelby's theoretical formulation for calculating the stress of an ellipsoidal inclusion by Finite Element Analysis by assuming suitable mathematical model in order to calculate the stress field. There seems to be a big gap between Eshelby's highly sophisticated method and a purely numerical method such as the finite element method and there is not much work done to the author's best knowledge that discusses the bridge between the purely theoretical work and purely numerical work. Combination of micromechanics with numerical approaches should open a new paradigm in today's solid mechanics research leading to better understanding of modern materials which did not exist before.

In this thesis, Chapter 2 presents the equivalent inclusion method and Eshelby's tensor In Chapter 3, discusses the finite element modeling of the matrix and inclusion .Finally in Chapter 4, conclusions and recommendations are presented.

CHAPTER 2

EQUIVALENT INCLUSION METHOD AND ESHELBY'S TENSOR

2.1INTRODUCTION

When the elastic modulus of an ellipsoidal subdomain in a material differs from that of the remainder (matrix), the sub domain is called an ellipsoidal inhomogeneity. Voids, cracks and precipitates are examples of the inhomogeneity which might also be called an inclusion.

A material containing inhomogeneities is free from any stress field unless a load is applied. On the other hand, a material containing inclusions is subjected to an internal stress (eigenstress) field, even though it is free from all external tractions. If an inhomogeneity contains an eigen strain, it is called an inhomogeneous inclusion. Most of the precipitates in alloys and martensites in phase transformation are inhomogeneous inclusions. Eigen strain inside these inhomogeneous inclusions are misfits and phase transformation strains.

Eshelby [1] first pointed out that this stress disturbance in an applied stress due to the presence of an in homogeneity can be simulated by an eigen stress caused by an inclusion when the eigen stress is chosen properly. This equivalency is called the equivalent inclusion method [4].

2.2 Equivalent Inclusion Method

Consider an infinitely extended material with the elastic module C^m containing an ellipsoidal domain Ω with the elastic modulus C^i .The domain Ω is called an ellipsoidal in homogeneity. We investigate the disturbance by the presence of this in homogeneity. Let us denote the applied stress at infinity as σ^0 and the corresponding strain as ε^0 .And the stain disturbance is denoted as ε

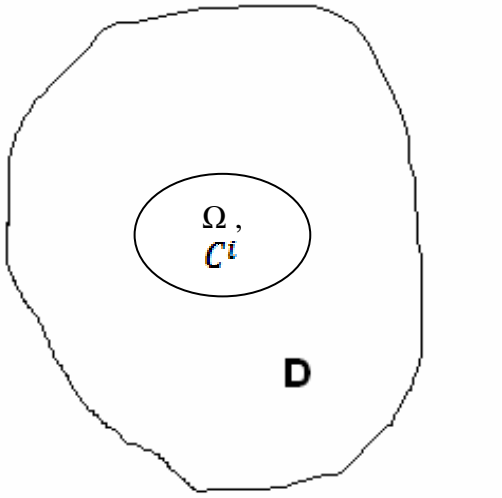

FIGURE 2.1 Inclusion C^i in a matrix C^m

Hooks Law for the above system is written as

$$\sigma^0 = C^i(\varepsilon^0 + \varepsilon) \quad \text{In } \Omega \text{ region} \tag{2.1}$$

$$\sigma^0 = C^m(\varepsilon^0 + \varepsilon) \text{ In D- } \Omega \text{ region} \tag{2.2}$$

The equivalent inclusion method is used to simulate the stress disturbance using the eigen stress resulting from an inclusion which occupies the space Ω.

Consider an infinitely extended homogeneous material with the elastic moduli C^m everywhere, containing the domain Ω with an eigen strain ε^*. The quantity ε^* has been introduced by use of the arbitrarily in order to simulate the in homogeneity problem by use of the inclusion method. Such an eigen strain is called an equivalent eigen strain. When this homogeneous material is subjected to the applied strain ε at infinity the resulting stress is σ .Then Hook's law yields

$$\sigma^0 = C^m(\varepsilon^0 + \varepsilon - \varepsilon^*) \text{ In } \Omega \tag{2.3}$$

$$\sigma^0 = C^m(\varepsilon^0 + \varepsilon) \text{ In D- } \Omega \text{ region} \tag{2.4}$$

The necessary and sufficient condition for the equivalency of the stresses and strains in the above two problems of the in homogeneity and inclusion

$$C^i(\varepsilon^0 + \varepsilon) = C^m(\varepsilon^0 + \varepsilon - \varepsilon^*) \text{ In } \Omega \text{ region} \tag{2.5}$$

By the above method ε can be obtained as a known function of ε^* when the eigen strain problem in the homogeneous material is solved. Thus (1.5) determines ε^* for a given ε, in such a manner that equivalency holds. After obtaining ε^*, the stress σ^0 can be found from (2.0) or (2.3)

If σ^0 is a uniform stress, ε^* is also uniform in Ω .Then

$$\varepsilon = \text{S } \varepsilon^* \tag{2.6}$$

S is called the Eshelbys tensor

Substitution of (2.6) into (2.5) leads to

$$C^i(\varepsilon^0 + S\varepsilon^*) = C^m(\varepsilon^0 + S\varepsilon^* - \varepsilon^*) \tag{2.7}$$

From which six unknowns ε^* is determined

2.3 Eshelby's Tensor

From equation (1.6) we equated elastic strain to eigenstrain with a factor S. It is called Eshelby's tensor. S is a fourth rank tensor and it depends on the ratio of the principal axes of a_1, a_2, a_3 and ν (Poisson's ratio)

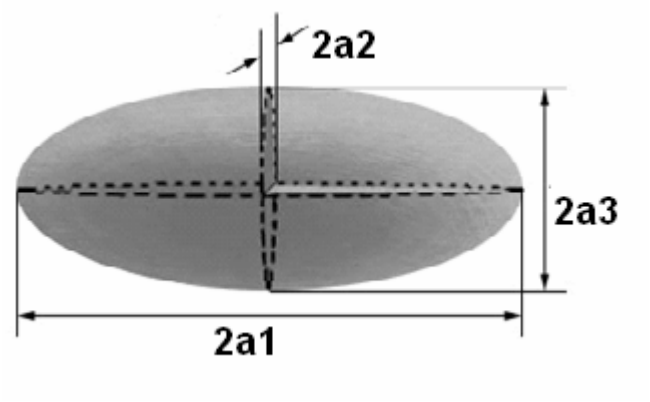

FIGURE 2.2 Ellipsoidal Inclusion with semi principle axes a_1, a_2, a_3

The components of S can be obtained from the following formula

$$S_{ijkl} = \frac{\varepsilon^*}{16\pi(1-\nu)} \sum \int \frac{\lambda_i g_{jmn} + \lambda_j g_{imn}}{g} d\omega \qquad (2.8)$$

The above formula was derived by the Green's function approach. Based on the above equivalent inclusion principle, we can validate the Eshelby's theorem by the finite element method.

CHAPTER 3

FINITE ELEMENT MODELING OF MATRIX AND INCLUSION

3.1 Introduction

The finite element method has become a popular technique for predicting the response of structures and materials. Finite element analysis software solves complex structures by breaking the structure into small elements. Established finite element software has long been commercially available for analyzing short time, small deformation behavior of structures with linear material and geometric properties. Until recently, nonlinear finite element analysis that would address structures which undergo short time, large deformations with nonlinear material and geometric properties were not commonly available.

The finite element analysis procedure used in this study is Ansys Workbench [8]. Initially a 3-D model of the matrix and inclusion is created in Pro-E Wildfire and it is exported to Ansys Workbench Simulation environment. The Ansys Workbench preprocessor was used to create and mesh the geometry. Once the mesh had been completed, the material and boundary condition were included in the analysis code and the system was solved iteratively. Upon convergence of the analysis code, the results were viewed using the Ansys Workbench post processing tool.

3.2 Modeling Steps of Matrix -Inclusion

3.2.1 Finite Element Modeling:

To start with a part CAD model of the matrix and inclusion is created in Pro E Wildfire and is assembled to form the matrix –inclusion set. The matrix is an infinite region and inclusion is very small volume of the entire matrix .Since infinite matrix is an assumption on which the theory is based, modeling an infinite region is impractical effort we solve this ambiguity by considering the matrix model to be a cube of dimension of 1000 x 1000 x 1000 meters and ellipsoidal inclusion dimension of 50 x 25 x 25 meters .The matrix dimension is very large compared to the inclusion dimension, and its size tends to infinity .This model is then exported to Ansys Workbench Simulation where the actual stress analysis is carried out.

We study the stresses inside the inclusion, when the matrix region is subjected to shear and normal forces on its boundary. Since the model is symmetric with respect to a plane passing through the mid –height, we can perform stress analysis on one fourth of the model, by doing so that the PC memory usage and also analysis run time are greatly reduced.

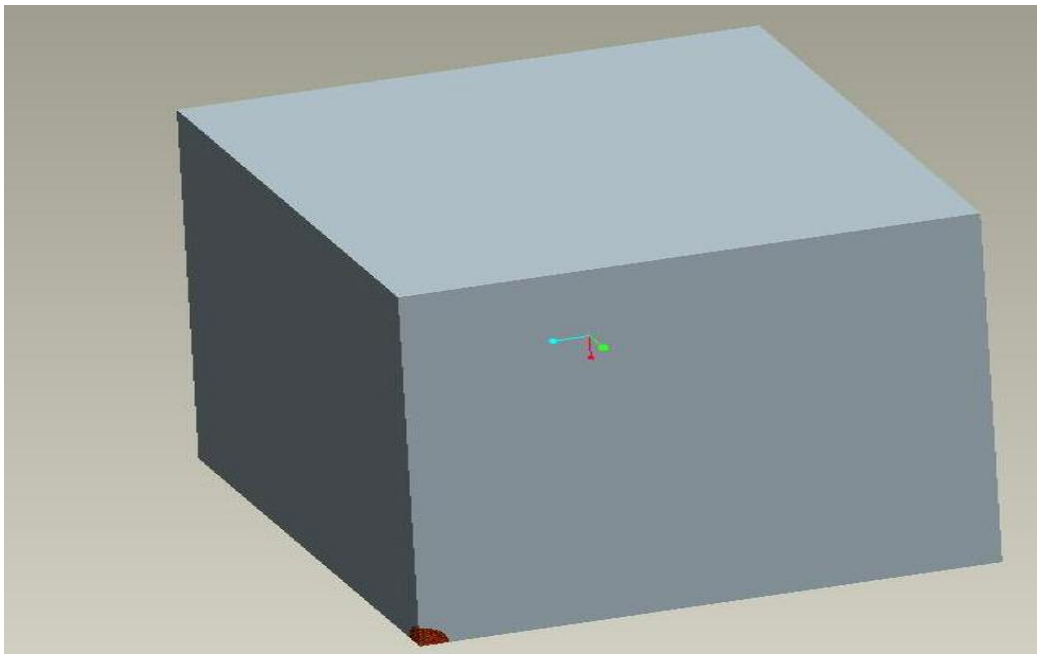

Figure 3.1 3-D CAD model of the matrix and inclusion (solid model)

3.2.2 Assigning Material Properties

The ellipsoidal inclusion is usually a stiffer material dispersed in a less comparatively stiffer matrix .Thus for the matrix region polyethylene is chosen and for inclusion cast iron is chosen. The following table gives the material properties and their values of the matrix –inclusion region.

3.1Table - Material Property of the matrix and Inclusion

Property	Matrix	Inclusion
E	2.25 G Pa	211 G Pa
υ	0.4	0.3

3.2.3 Defining the Contact Element

Since the efficiency of the fiber reinforcement is directly related to the high interfacial shear strength at the interfaces between the fibers and the polymer matrix, the ideal interfacial bond should be strong enough to hold the inclusion and to achieve this strong bond we define the contact between the matrix and inclusion as bonded contact. This is the default configuration for contact regions. If contact regions are bonded, then no sliding or separation between faces or edges is allowed. Think of the region as *glued*. This type of contact allows for a linear solution since the contact length/area will not change during the application of the load. If contact is determined on the mathematical model, any gaps will be closed and any initial penetration will be ignored.

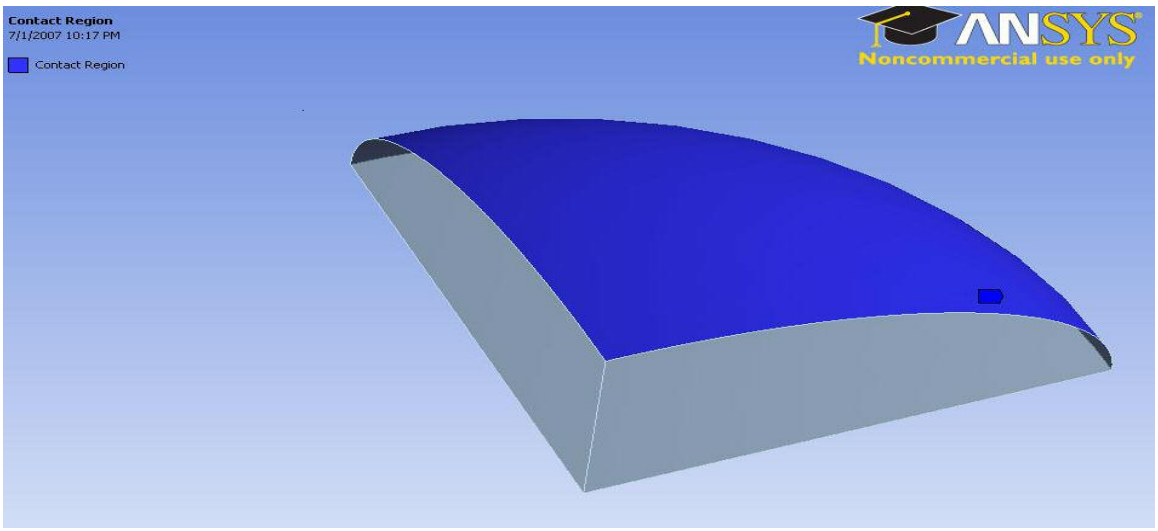

Figure 3.2 Bonded contact region of the inclusion

3.2.4 Meshing

A key step in any numerical calculation is mesh generation. Workbench simulation automatically develops a finite element mesh appropriate to the problem. Default mesh

that is created consists of 127 three dimensional brick elements and is shown in the next figure.

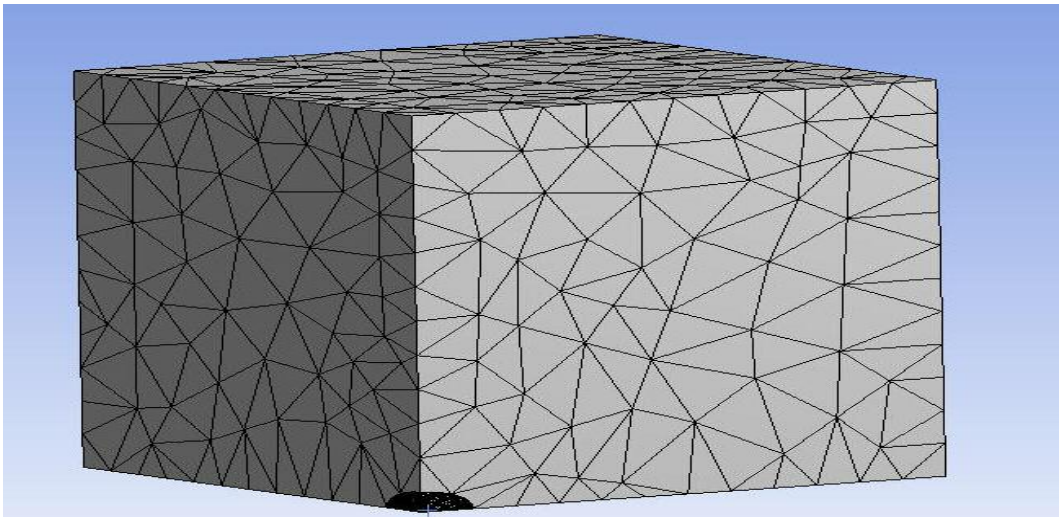

Figure 3.3 Meshed matrix and inclusion region

3.2.5 Mesh Refinement of the Inclusion

The inclusion region is the region where the most interest lies as we analyze the stress and strain effects in this region .In order to get higher accurate results in this region we refine the mesh to finer mesh and as the matrix region is of less significance for stress and strain effects we mesh it with coarse mesh.

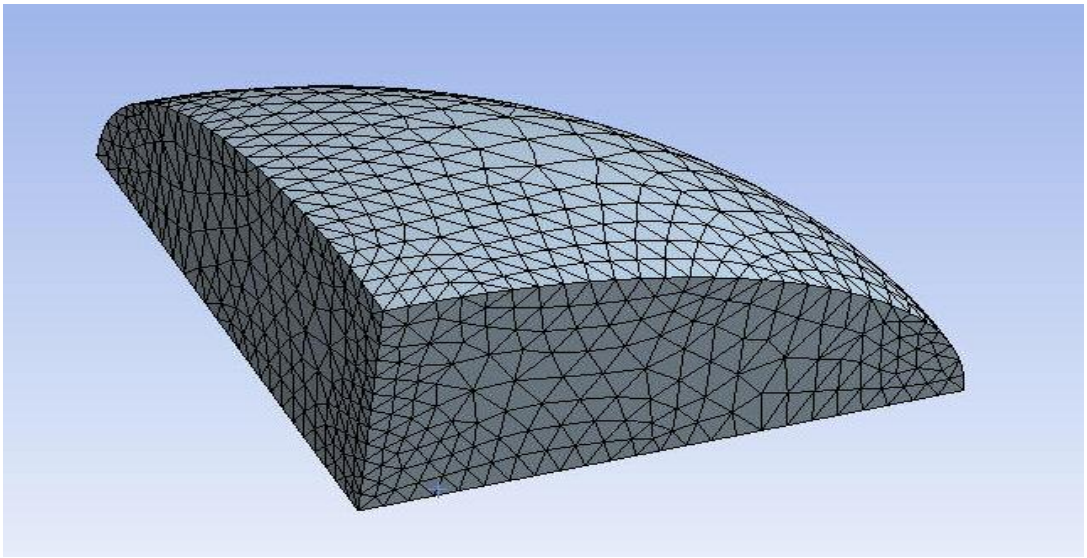

Figure 3.4 Finer mesh refined inclusion region

3.2.6 Applying Loads and Displacements

The symmetric nature of geometry and loading means that displacements are zero in directions normal to the faces exposed by the vertical and horizontal plane employed to create this one-fourth segment of the cube. The normal and shear force is applied on the top surface of the cube and on the remaining three planes which pass along the XY, YZ and ZX, the displacements are in the Z, X and Y direction are set to zero respectively. This boundary condition is necessary to restrain the rigid body motion of the model so that when we apply load we get elastic deformation not a rigid body movement.

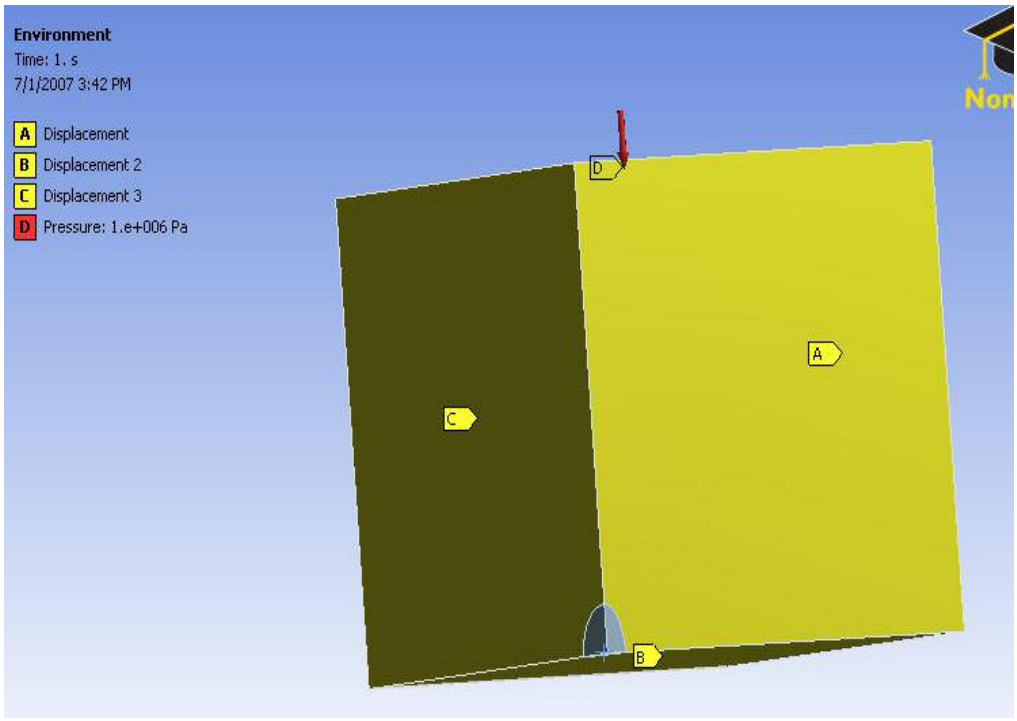

Figure 3.5 Loading and displacements on the matrix region

The post processing and validation of the results are discussed in the next chapter.

CHAPTER 4

MATHEMATICAL AND FINITE ELEMENT MODELING OF ELLIPSOIDAL INCLUSION

4.1Introduction

This chapter deals with analytical and finite element model that will be used to predict the stress disturbance in the ellipsoidal inclusion. The mathematical model is based on the equivalent inclusion model that was developed by J D Eshelby [1] to predict the elastic field in an ellipsoidal inclusion. The FEM model is developed based on thee continuum mechanics approach. The stress inside the ellipsoid calculated by the theoretical model is compared with values that are obtained by the FEM model. The comparison is made for different aspect ratios of the ellipsoid and different elastic modulus of the inclusion.

4.2 Mathematical Modeling

Before going any further into the analysis we have to choose the material properties for the matrix and inclusion. We choose the elastic modulus of the matrix and inclusion to be 211 G Pa & 2.25 G Pa respectively. These values are chosen to simulate carbon/epoxy (replace with actual materials). The following table gives the values of the material properties used and their values that are assigned for the inclusion and matrix region.

Table 4.1-Material properties of Matrix and Inclusion

Property	Matrix	Inclusion
E	2.25 G Pa	211 G Pa
ν	0.4	0.3
λ	3.633 G Pa	121.65 G Pa
μ	0.865 G Pa	81.153 G Pa

Here λ and μ are Lames constant and depend on E and ν by the following relation:

$$\lambda = \frac{E\nu}{(1+\nu)(1-2\nu)} \tag{4.1}$$

$$\mu = \frac{E}{2(1+\nu)} \tag{4.2}$$

To begin with the matrix is assumed to be an infinite region with a centrally located ellipsoidal inclusion. First the stress analysis is done for the shear component namely the σ_{12} component for spherical $(a_1 = a_2 = a_3)$ and for a prolate spheroid $(a_1 > a_2 = a_3)$ where a_1, a_2, a_3 being the principal half axes of the ellipsoidal inclusion. Next the stress analysis is carried out in σ_{23} component for the prolate spheroid and finally the σ_{11}, σ_{22} and σ_{33} components in the shear and normal directions are validated for spherical and prolate spheroid.

In order to measure the stress disturbance in the inclusion the equivalent inclusion method is used. In the index notation form the equation (1.6) and (1.7) can be rewritten as

$$C^m_{ijkl}(\varepsilon^0_{kl} + \varepsilon_{kl}) = C^i_{ijkl}(\varepsilon^0_{kl} + \varepsilon_{kl} - \varepsilon^*_{kl}) \tag{4.3}$$

$$\varepsilon_{kl} = S_{klmn}\varepsilon^*_{kl} \tag{4.4}$$

Where

C^i_{ijkl}, is a fourth rank tensor denotes the elastic modulas of the inclusion

C^m_{ijkl}, is a fourth rank tensor denotes the elastic modulas of the matrix

ε^0_{kl}, is elastic strain at infinity

ε_{kl}, is elastic strain

ε^*_{kl}, is the eigen strain

S_{klmn}, is a fourth rank tensor and is the Eshelbys tensor

4.3 Shear Stress Validation for a Spherical Inclusion.

4.3.1 Mathematical Model

The Eshelby's tensor for a spherical inclusion with principle axis a_1, a_2, a_3 ($a_1 = a_2 = a_3$) is given by the following relation.

$$S_{1212} = \frac{4 - 5\nu}{15(1-\nu)} \tag{4.5}$$

Substituting ν =0.4, in the above equation relation

$$S_{1212} = 0.222 \tag{4.6}$$

Next to calculate the stress in the inclusion we go back to equation (4.3) and rewrite for the 1212 component of stresses it becomes

$$C^m_{1212}(\varepsilon^0_{12}+\varepsilon_{12}) = C^i_{1212}(\varepsilon^0_{12}+\varepsilon_{12}-\varepsilon^*_{12}) \tag{4.7}$$

Along with

$$\varepsilon_{12} = S_{1212}\varepsilon^*_{12} \tag{4.8}$$

Since 1212 is repeated, applying the summation convention

$$\varepsilon_{12} = 2S_{1212}\varepsilon^*_{12} \tag{4.9}$$

Substituting equation (4.9) into equation (4.7) and simplifying further it gives

$$\varepsilon^*_{12} = \frac{C^i_{1212}-C^m_{1212}}{2(C^m_{1212}-C^i_{1212})S_{1212}-C^m_{1212}}\varepsilon^0_{12} \tag{4.10}$$

The elastic module for isotropic materials is given by

$$C_{ijkl} = \lambda\delta_{ij}\delta_{kl}+\mu\delta_{jk}\delta_{jl}+\mu\delta_{il}\delta_{jk} \tag{4.11}$$

- δ is Kronecker's delta which is defined as

$$\delta_{ij} = \begin{Bmatrix} 1 \rightarrow if\,(i,j) = (1,1),(2,2),(3.3) \\ 0 \rightarrow otherwise \end{Bmatrix} \tag{4.12}$$

Using the above identity and writing it for 1212 component equation (4.11) becomes

$$C_{1212} = \lambda\delta_{12}\delta_{12}+\mu\delta_{12}\delta_{12}+\mu\delta_{12}\delta_{12} \tag{4.13}$$

$$C_{1212} = \lambda\times 0+\mu\times 1\times 1+\mu\times 0 \tag{4.14}$$

$$C_{1212} = \mu \tag{4.15}$$

From table (4.1) the value of μ from the inclusion and matrix region is listed, using those

$$C^{i}_{1212} = \mu^{i} = 211 \text{ G Pa} \tag{4.16}$$

$$C^{m}_{1212} = \mu^{m} = 2.25 \text{ G Pa} \tag{4.17}$$

Substituting the above and the value of S_{1212} into equation (4.7) we obtain ε^{*}_{12} in terms of ε^{0}_{12}

$$\varepsilon^{*}_{12} = -2.198\, \varepsilon^{0}_{12} \tag{4.18}$$

The equation to calculate the stress inside the inclusion is given by

$$\sigma_{12} = C_{1212}(\varepsilon^{0}_{12} + 2S_{1212}\, \varepsilon^{*}_{12} - \varepsilon^{*}_{12}) \tag{4.19}$$

This equation is used in calculating the value of stress inside the inclusion with the ε^{0}_{12} obtained from the Ansys Workbench Simulation results.

4.3.2 Finite Element Model of the Spherical Inclusion

The finite element modeling of the spherical inclusion is carried out on the same steps that was discussed in chapter 3 except here the inclusion is spherical inclusion of principal axis 25 x 25 x 25 meters($a_1 = a_2 = a_3$) and a shear force of 10 M Pa is applied on the top surface of the cube. The loading and displacement conditions that was discussed earlier is followed .The following figure shows the FEM model of the spherical inclusion

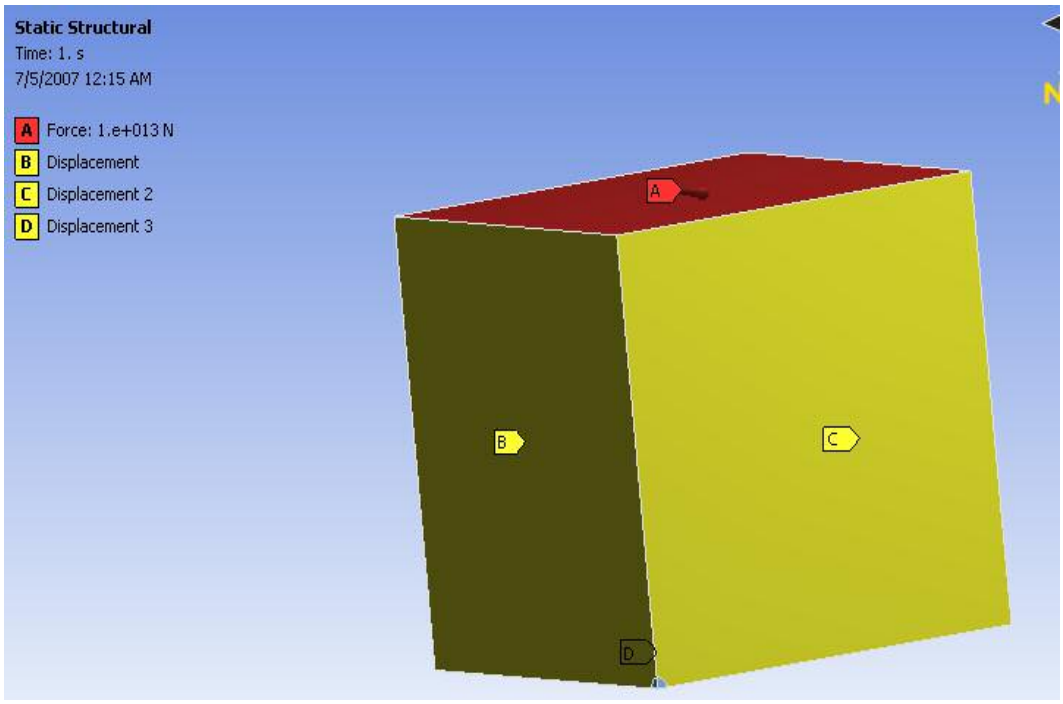

Figure 4.1 FEA model of the matrix -spherical inclusion

Shear stress validation

From equation (4.19) we have

$$\sigma_{12} = C^{m}_{1212}(\varepsilon^{0}_{12} + 2S_{1212}\ \varepsilon^{*}_{12} - \varepsilon^{*}_{12}), \tag{4.20}$$

Substituting the values of C^{m}_{1212}, S_{1212} and ε^{*}_{12} from equation ( ), () and () we arrive at

$$\sigma_{12} = 4.9996 \text{ x } 10^{9}\ \ \varepsilon^{0}_{12} \tag{4.21}$$

In the above equation the unknown factor is ε^{0}_{12}, for this go back to our Ansys simulation post processing results to find the value of ε^{0}_{12}

4.3.3 Ansys Post Processing

In post processing we try to evaluate the strain ε^{0}_{12}, which is the strain at infinity in the matrix-inclusion model and stress σ_{12} in the inclusion region .The numerically

obtained ε_{12}^{0} is then substituted in equation (4.21) in order to find the σ_{12} mathematically and this value is compared with the numerically obtained σ_{12} .The following figure shows the shear strain values obtained from FEA

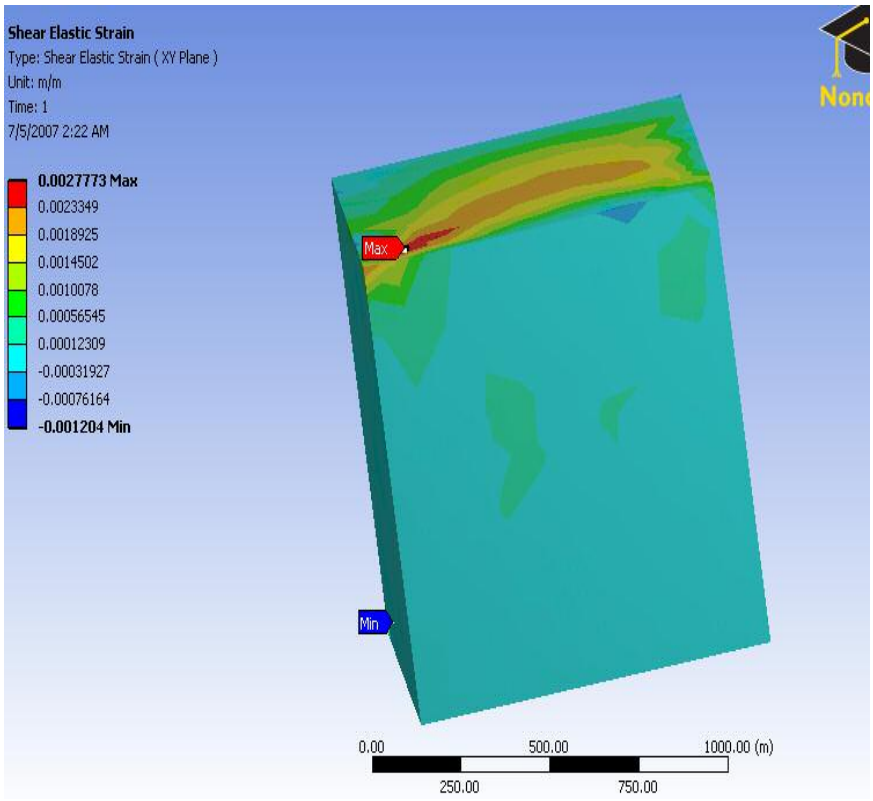

Figure 4.2 Strain plot of the spherical inclusion analysis

The above figure shows the strain plot in the 12 i.e. XY component and the maximum value is 0.002773, this corresponds to ε_{12}^{0}. Substituting ε_{12}^{0} =0.002773 in equation (4.21) we obtain σ_{12} =13.65 M Pa and a constant numerical σ_{12} value as 13.57 M Pa as shown by the below shear stress plot in the inclusion region.

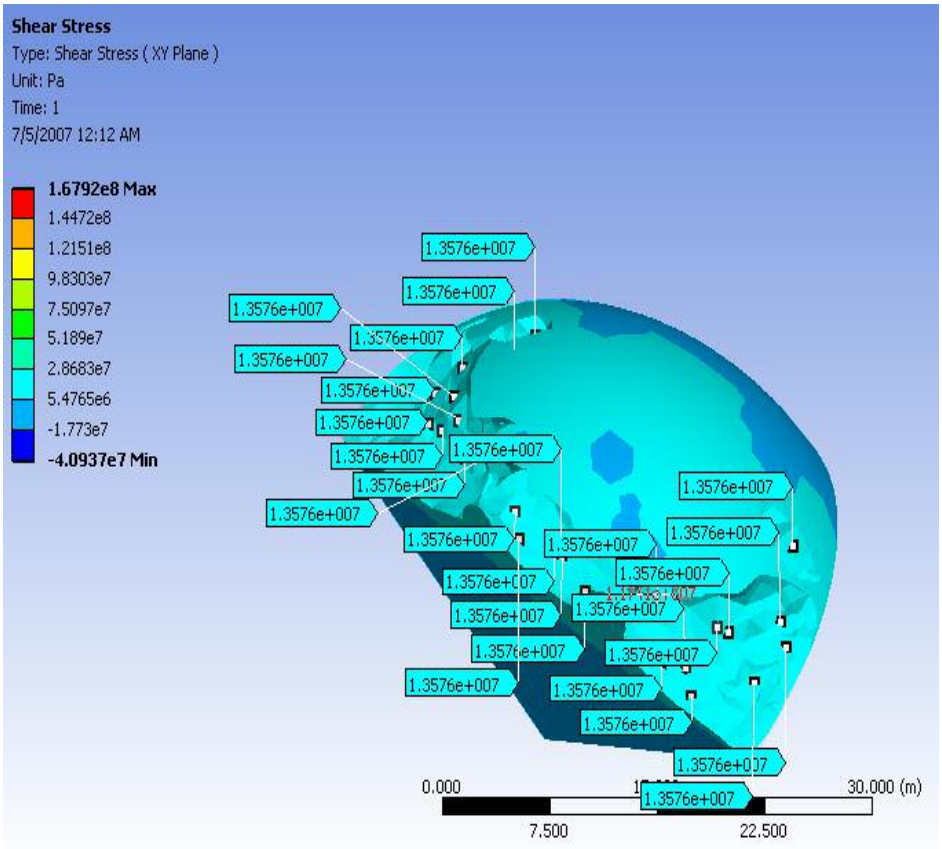

Figure 4.3 Stress plot of the spherical inclusion

From the figure above we can see that the stress inside the inclusion is constant for any point inside the entire volume .This predicts the validity of J D Eshelbys constant stress in the inclusion for constant strain at infinity in the matrix. Therefore by the above analysis we could validate J D Eshelbys constant stress theorem and also evaluate the mathematically obtained stress with numerically obtained one .As the inclusion property changes i.e. .e we make it more stiffer than the matrix material by increasing the young's modulas of the inclusion we notice that the stress inside the inclusion also increases .The following table gives different ratio of young's modulas of matrix and inclusion and the ratio of outside stress to inclusion stresses .

Table 4.2 Shear Stress Validation for different ratio Matrix –Inclusion E values

$\frac{E_m}{E_I}$	σ_∞ (M Pa)	σ_{12} (M Pa)	$\frac{\sigma_\infty}{\sigma_{12}}$
$\frac{1}{5}$	10	14.797	0.6758
$\frac{1}{10}$	10	17.125	0.5839
$\frac{1}{20}$	10	19.231	0.5199
$\frac{1}{50}$	10	24.156	0.4139
$\frac{1}{100}$	10	28.100	0.3558

4.4 Shear Stress Validation for Spherical Inclusion along the 12 Direction.

Validation of the shear stresses for a spherical inclusion was the first step in our analysis of the ellipsoidal inclusion. Next, we move our attention towards an inclusion which is of ellipsoidal shape. The analysis of the ellipsoidal region is important as the most shapes of the inclusion in the matrix region can be approximated by an ellipsoid. For an ellipsoidal inclusion, the mathematical and FEM models are carried out using the same steps as discussed in Chapter 3. In this section, we try to validate the shear stress

for the 12 component. For an ellipsoidal inclusion of prolate ellipsoidal shape ($a_1 > a_2 = a_3$), the Eshelby's tensor is given by

$$S_{1212} = \frac{a_1^2 + a_2^2}{16\pi(1-\nu)} I_{12} + \frac{1-2\nu}{16\pi(1-\nu)}(I_1 + I_2) \tag{4.22}$$

Where I_1, I_2 and I_{12} the standard elliptical integrals (Gradshteyn and Ryzhik, 1965), assuming $a_1 > a_2 > a_3$, as

$$I_1 = \frac{4\pi a_1 a_2 a_3}{(a_1^2 - a_2^2)(a_1^2 - a_3^2)^{1/2}} \left\{ F(\theta,k) - E\left(\theta,k\right) \right\}, \tag{4.23}$$

$$I_3 = \frac{4\pi a_1 a_2 a_3}{(a_2^2 - a_3^2)(a_1^2 - a_3^2)^{1/2}} \left\{ \frac{a_2 (a_1^2 - a_3^2)^{1/2}}{a_1 a_3} - E\left(\theta,k\right) \right\}, \tag{4.24}$$

Where

$$F(\theta,k) = \int_0^\theta \frac{dw}{(1 - k^2 \sin^2 w)^{1/2}}, \tag{4.25}$$

$$E\left(\theta,k\right) = \int_0^\theta (1 - k^2 \sin^2 w)^{1/2} dw, \tag{4.26}$$

$$\theta = \sin^{-1}(1 - a_3^2 / a_1^2)^{1/2}, \tag{4.27}$$

$$k = \left\{ (a_1^2 - a_2^2) / (a_1^2 - a_3^2) \right\}^{1/2}. \tag{4.28}$$

And the remaining integrals are defined by

$$\begin{aligned} &I_1 + I_2 + I_3 = 4\pi \\ &3I_{11} + I_{12} + I_{13} = 4\pi / a_1^2, \\ &3a_1^2 I_{11} + a_2^2 I_{12} + a_3^2 I_{13} = 3I_1, \\ &I_{12} = \left(I_2 - I_1\right) / (a_1^2 - a_2^2). \end{aligned} \tag{4.29}$$

For equation (4.22), substituting ν=0.4 and the principal axes of $a_1 = 50, a_2 = 25, a_3 = 25$, and I_1, I_2 and I_{12} defined by the following formula

$$I_2 = \frac{2\pi a_1 a_3^2}{(a_1^2 - a_3^2)^{3/2}} \left\{ \frac{a_1}{a_3} \left(\frac{a_1^2}{a_3^2} - 1 \right)^{1/2} - \cos^{-1} h \frac{a_1}{a_3} \right\} \tag{4.30}$$

$$I_1 = 4\pi - 2I_2 \ , \tag{4.31}$$

$$I_{12} = (I_2 - I_1)/(a_1^2 - a_2^2) \tag{4.32}$$

Substituting $a_1 = 50, a_2 = 25, a_3 = 25$ in the above equations we obtain

$$I_2 = 5.19265 \tag{4.33}$$

$$I_1 = 2.18107 \tag{4.34}$$

$$I_{12} = 0.00160618 \tag{4.35}$$

Substituting the above I values in equation (4.22), we obtain

$$S_{1212} = 0.2153 \tag{4.36}$$

Substituting the above and the value of S_{1212} into equation (4.7) we obtain ε_{12}^* in terms of ε_{12}^0 as

$$\varepsilon_{12}^* = -2.26537\, \varepsilon_{12}^0 \tag{4.37}$$

The stress inside the ellipsoidal inclusion is given by the

$$\sigma_{12} = C_{1212}^m (\varepsilon_{12}^0 + 2S_{1212}\, \varepsilon_{12}^* - \varepsilon_{12}^*), \tag{4.38}$$

Using the equation, and substituting the value of S_{1212} from equation (4.36) we obtain

$$\sigma_{12} = 5.1522 \times 10^9 \varepsilon_{12}^0 \tag{4.39}$$

To find the stress using above relation we need ε_{12}^{0} and ε_{12}^{0} is found from ansys simulation

4.4.1 Finite Element Model of the Ellipsoidal inclusion

The finite element modeling of the ellipsoidal inclusion is carried out using the same steps that were discussed in Chapter 3 except here that the inclusion is of prolate shape with the principal axes of 50 x 25 x 25 meters ($a_1 > a_2 = a_3$) and a shear force of 10 M Pa being applied on the top surface of the cube. The loading and displacement conditions that were discussed earlier are followed. The following figure shows the ellipsoidal inclusion and the FEA model.

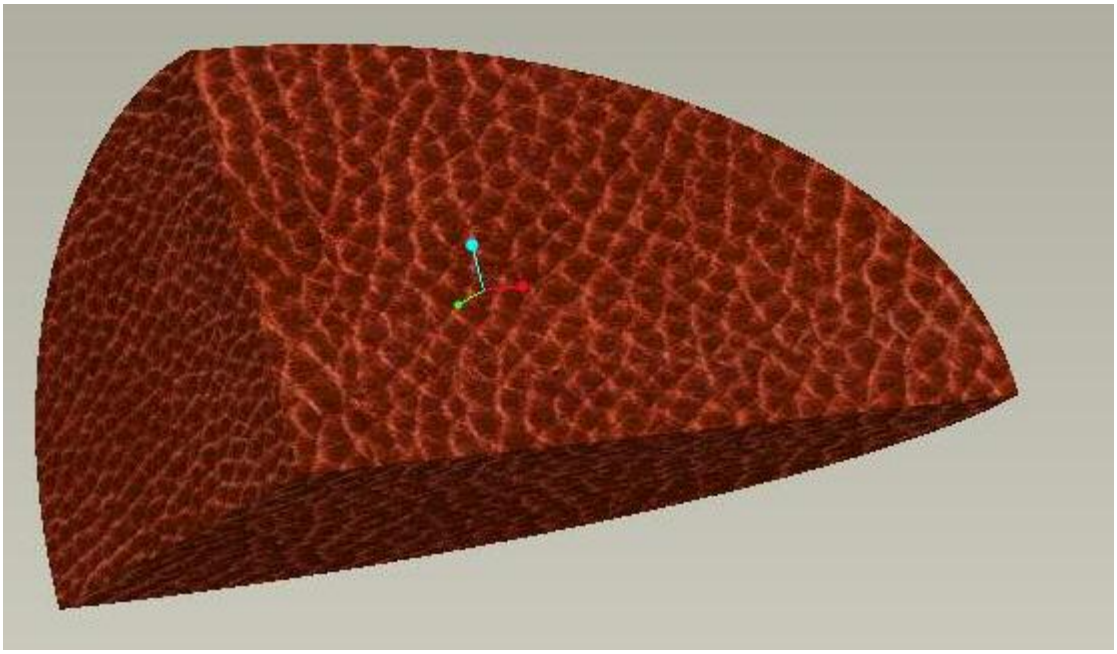

Fig 4.4 The Ellipsoidal Inclusion

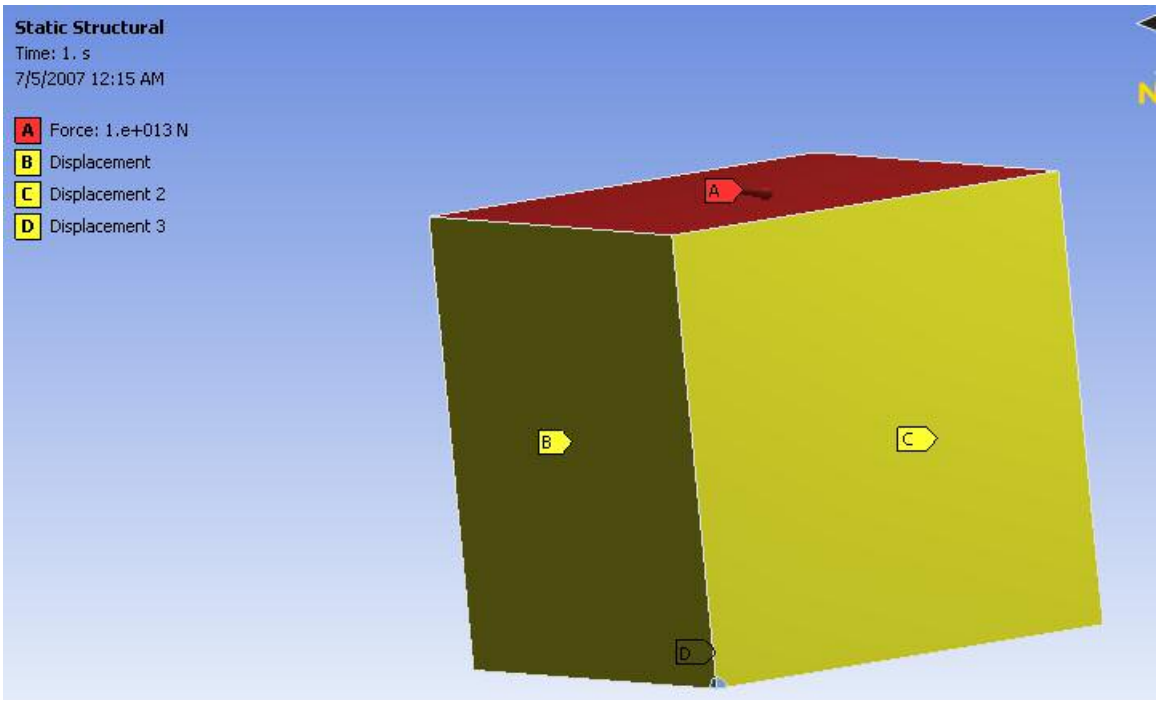

Fig 4.5 FEA model of the matrix and ellipsoidal inclusion

4.4.2Ansys Post Processing

For the stress σ_{12}^{0} = 10 MPa that is applied at infinity on the matrix boundary, we obtain the corresponding ε_{12}^{0} strain at infinity. This value is numerically obtained from the strain plot curve obtained by the Ansys simulation post processing result. The following plot shows it.

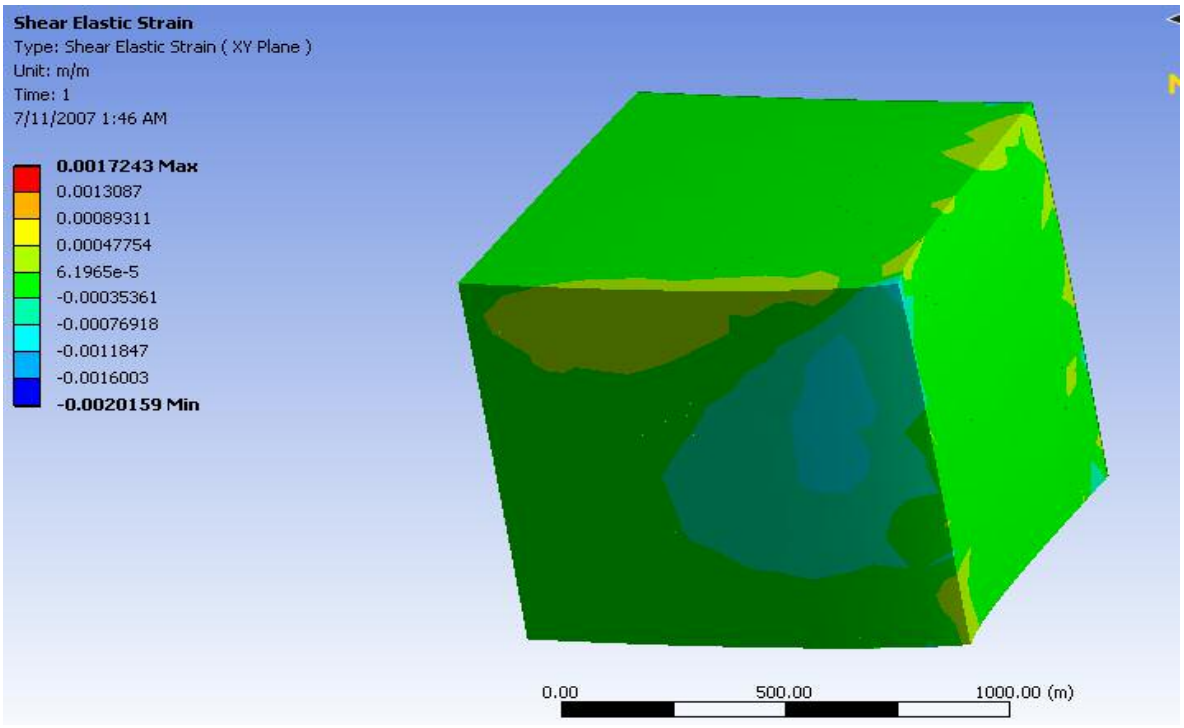

Fig 4.6 The strain plot of the matrix and ellipsoidal inclusion

The above figure shows the strain plot in the 12 i.e. XY component and the maximum value is 0.0017243, this corresponds to ε_{12}^{0}. Substituting ε_{12}^{0} =0.001724373 in equation ( ) we obtain σ_{12} =8.90 M Pa and a constant numerical σ_{12} value as 9.022 M Pa as shown by the below shear stress plot in the inclusion region. We are able to get close approximated result from the numerical analysis converging with the theoretical result.

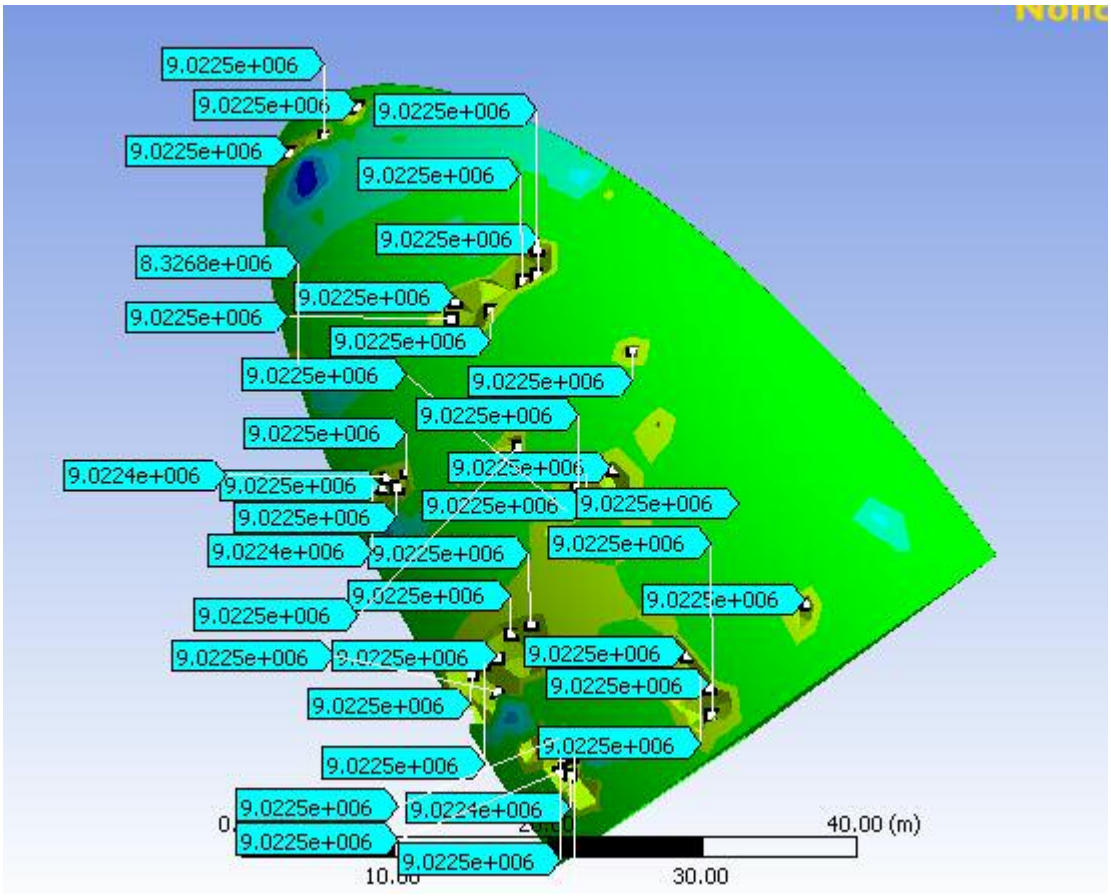

Fig 4.7 Stress plot of the inclusion region

As we change the aspect ratio of the ellipsoidal inclusion and subject it to the same loading and boundary conditions, *i.e*., if we increase the ratio of a_1 axes to ratio of a_2 axis monotonically from 2, 5 upto 100, we see that the stress inside the ellipsoidal inclusion decreases with the aspect ratio and then becomes constant when the ellipsoid shape approximates itself to a cylinder. The following table gives the S values, strain values and stress values obtained for different aspect ratios of the ellipsoidal inclusion

Table 4.3 The Stress, Strain and S values for different aspect ratios. (12 component)

Aspect ratio $\left(\frac{a_1}{a_2}\right)$	S	ε_{12}^{*}	ε_{12}^{0}	$\sigma_{12}(theory)$ MPa	$\sigma_{12}(ansys)$ MPa
2	0.2153	-2.2653 ε_{12}^{0}	0.0017243	8.8836	9.0225
5	0.2318	-2.1072 ε_{12}^{0}	0.0017175	8.2308	8.1243
10	0.2421	-2.0201 ε_{12}^{0}	0.0017067	7.8410	8.1032
20	0.2470	-1.9803 ε_{12}^{0}	0.0016282	7.3332	7.9196
50	0.2493	-1.9629 ε_{12}^{0}	0.001553	6.9331	6.6790
100	0.2497	-1.9594 ε_{12}^{0}	0.001367	6.0915	6.0127

4.5 Shear Stress Validation for Spherical Inclusion along the 23 Direction

In the previous section, we validated the stresses in the 12 directions. Now we will analyze the stresses in the 23 direction for an ellipsoidal inclusion of prolate shape ($a_1 > a_2 = a_3$). The Eshelby tensor for the 2323 component is given by

$$S_{2323} = \frac{a_2^2 + a_3^2}{16\pi(1-\nu)} I_{23} + \frac{1-2\nu}{16\pi(1-\nu)}(I_2 + I_3) \tag{4.40}$$

The quantities, I_2, I_3 and I_{23}, are defined by the following formulae :

$$I_2 = I_3 = \frac{2\pi a_1 a_3^2}{(a_1^2 - a_3^2)^{3/2}} \left\{ \frac{a_1}{a_3} \left(\frac{a_1^2}{a_3^2} - 1 \right)^{1/2} - \cos^{-1} h \frac{a_1}{a_3} \right\} \tag{4.41}$$

$$I_{23} = \frac{\pi}{a_2^2} - \frac{(I_2 - I_1)}{4(a_1^2 - a_2^2)} \tag{4.42}$$

$$I_1 = 4\pi - 2I_2 \tag{4.43}$$

Substituting the value of principal axes $a_1 = 50, a_2 = 25, a_3 = 25$, in the above integrals, the value becomes

$$I_2 = I_3 = 5.19265 \tag{4.44}$$

$$I_1 = 2.18107 \tag{4.45}$$

$$I_{23} = 0.004625 \tag{4.46}$$

Putting these back into equation (4.40) we obtain

$$S_{2323} = 0.2605 \tag{4.47}$$

And the equation ε_{12}^* in terms ε_{23}^0 would result in

$$\varepsilon_{23}^* = -2.26537\, \varepsilon_{23}^0 \tag{4.48}$$

Substituting equations (4.46) and (4.47) in equivalent inclusion equation we obtain

$$\sigma_{12} = 4.27572 \times 10^{9} \varepsilon_{23}^{0} \qquad (4.49)$$

As we did in earlier two cases, we use Ansys simulation result to obtain ε_{23}^{0}

4.5.1 Ansys Post Processing

For the stress σ_{23}^{0} = 10 M Pa that is applied at infinity on matrix boundary we obtain corresponding ε_{23}^{0} strain at infinity, this value is numerically obtained from the strain plot curve obtained by the Ansys simulation post processing result. The following plot shows it.

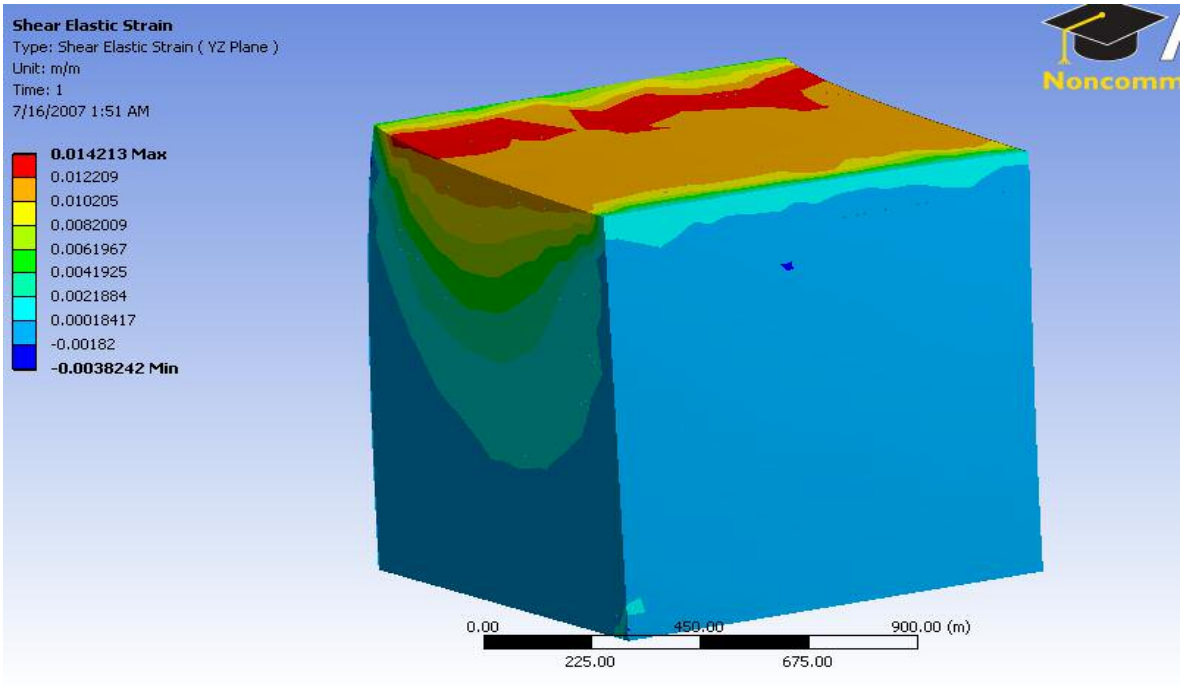

Figure 4.8 The stress plot in 23 directions

The above figure shows the strain plot in the 23 direction, *i.e.*, the YZ component and the maximum value is 0.014123, which corresponds to ε_{23}^{0}. Substituting

ε_{23}^{0}=0.014123 in equation (4.48), we obtain σ_{23}^{0}=60.37 MPa and a constant numerical σ_{23}^{0} value as 57.629 MPa numerically. We are able to get a closely approximated result from the numerical analysis converging with the theoretical result.

As we change the aspect ratio of the ellipsoidal inclusion and subject it same loading and boundary conditions, i.e. if we increase the ratio of a_1 axes to ratio of a_2 axis monotonically from 2, 5 so on to 100 we see that the stress inside the ellipsoidal inclusion decreases with aspect ratio and then becomes constant when the ellipsoid shape approximates itself to a cylinder. The following table gives the S values, strain values and stress values obtained for different aspect ratios of the ellipsoidal inclusion.

Table 4.4 The Stress, Strain and S values for different aspect ratios (23 components)

Aspect ratio $\left(\frac{a_1}{a_2}\right)$	S	ε_{23}^{*}	ε_{23}^{0}	$\sigma_{23}(theory)$ MPa	$\sigma_{23}(ansys)$ MPa
2	0.2605	-1.8800 ε_{23}^{0}	0.0141213	60.37	57.629
5	0.2834	-1.7313 ε_{23}^{0}	0.014103	55.53	52.009

Table 4.4-Continued

10	0.2889	-1.6985 ε_{23}^0	0.014175	54.75	51.0354
20	0.2908	-1.6878 ε_{23}^0	0.0141016	53.80	49.476
50	0.2915	-1.6841 ε_{23}^0	0.013997	53.609	49.342
100	0.2916	-1.6834 ε_{23}^0	0.013962	53.454	49.126

4.6 Normal stress validation for an ellipsoidal inclusion

In the previous sections, we validated the shear stress for a spherical and ellipsoidal inclusions. Now we come to the most important part of the analysis, *i.e.*, validating the stresses in the normal direction. The equations (4.3) and (4.4) can be written in the index notation for normal components in the11, 22 and 33 directions as

$C_{1111}^m(\varepsilon_{11}^0 + \varepsilon_{11}) = C_{1111}^i(\varepsilon_{11}^0 + \varepsilon_{11} - \varepsilon_{11}^*)$ along 11 direction (1.1)

$C_{2222}^m(\varepsilon_{22}^0 + \varepsilon_{22}) = C_{2222}^i(\varepsilon_{22}^0 + \varepsilon_{22} - \varepsilon_{22}^*)$ along 22 direction (1.2)

$C_{3333}^m(\varepsilon_{33}^0 + \varepsilon_{33}) = C_{3333}^i(\varepsilon_{33}^0 + \varepsilon_{33} - \varepsilon_{33}^*)$ along 33 direction (4.52)

And

$\varepsilon_{11} = S_{1111}\varepsilon_{11}^*$ (4.53)

$$\varepsilon_{22} = S_{2222}\varepsilon_{22}^{*} \tag{4.54}$$

$$\varepsilon_{33} = S_{3333}\varepsilon_{33}^{*} \tag{4.56}$$

Substituting the equations (4.52), (4.53) and (4.54) in equation (4.49), (4.50) and (4.51) respectively and applying the summation convention rule to the three simultaneous equations would lead to

$$\begin{aligned}
&C_{1111}^{i}\varepsilon_{11}^{0} + C_{1111}^{i}\varepsilon_{22}^{0} + C_{1111}^{i}\varepsilon_{33}^{0} + C_{1111}^{i}S_{1111}\varepsilon_{11}^{0} + C_{1122}^{i}S_{2211}\varepsilon_{11}^{*} + C_{1133}^{i}S_{3311}\varepsilon_{11}^{*} + \\
&C_{1111}^{i}S_{1122}\varepsilon_{11}^{*} + C_{1122}^{i}S_{2222}\varepsilon_{11}^{*} + C_{1133}^{i}S_{3322}\varepsilon_{11}^{*} + C_{1111}^{i}S_{1133}\varepsilon_{11}^{*} + C_{1122}^{i}S_{2233}\varepsilon_{11}^{*} + \\
&C_{1133}^{i}S_{3333}\varepsilon_{11}^{*} = C_{1111}^{m}\varepsilon_{11}^{0} + C_{1111}^{m}\varepsilon_{22}^{0} + C_{1111}^{m}\varepsilon_{33}^{0} + C_{1111}^{m}S_{1111}\varepsilon_{11}^{*} + C_{1122}^{m}S_{2211}\varepsilon_{11}^{*} + \\
&C_{1133}^{m}S_{3311}\varepsilon_{11}^{*} + C_{1111}^{m}S_{1122}\varepsilon_{11}^{*} + C_{1122}^{m}S_{2222}\varepsilon_{11}^{*} + C_{1133}^{m}S_{3322}\varepsilon_{11}^{*} + C_{1111}^{m}S_{1133}\varepsilon_{11}^{*} + \\
&C_{1122}^{m}S_{2233}\varepsilon_{11}^{*} + C_{1133}^{m}S_{3333}\varepsilon_{11}^{*} - C_{1111}^{m}\varepsilon_{11}^{*} - C_{1122}^{m}\varepsilon_{22}^{*} - C_{1133}^{m}\varepsilon_{33}^{*}
\end{aligned} \tag{4.57}$$

$$\begin{aligned}
&C_{2211}^{i}\varepsilon_{11}^{0} + C_{2222}^{i}\varepsilon_{22}^{0} + C_{2233}^{i}\varepsilon_{33}^{0} + C_{2211}^{i}S_{1111}\varepsilon_{11}^{0} + C_{2222}^{i}S_{2211}\varepsilon_{11}^{*} + C_{2233}^{i}S_{3311}\varepsilon_{11}^{*} + \\
&C_{2211}^{i}S_{1122}\varepsilon_{11}^{*} + C_{2222}^{i}S_{2222}\varepsilon_{11}^{*} + C_{2233}^{i}S_{3322}\varepsilon_{11}^{*} + C_{2211}^{i}S_{1133}\varepsilon_{11}^{*} + C_{2222}^{i}S_{2233}\varepsilon_{11}^{*} + \\
&C_{2233}^{i}S_{3333}\varepsilon_{11}^{*} = C_{2211}^{m}\varepsilon_{11}^{0} + C_{2222}^{m}\varepsilon_{22}^{0} + C_{2233}^{m}\varepsilon_{33}^{0} + C_{2211}^{m}S_{1111}\varepsilon_{11}^{*} + C_{2222}^{m}S_{2211}\varepsilon_{11}^{*} + \\
&C_{2233}^{m}S_{3311}\varepsilon_{11}^{*} + C_{2211}^{m}S_{1122}\varepsilon_{11}^{*} + C_{2222}^{m}S_{2222}\varepsilon_{11}^{*} + C_{2233}^{m}S_{3322}\varepsilon_{11}^{*} + C_{2211}^{m}S_{1133}\varepsilon_{11}^{*} + \\
&C_{2222}^{m}S_{2233}\varepsilon_{11}^{*} + C_{2233}^{m}S_{3333}\varepsilon_{11}^{*} - C_{2211}^{m}\varepsilon_{11}^{*} - C_{2222}^{m}\varepsilon_{22}^{*} - C_{2233}^{m}\varepsilon_{33}^{*}
\end{aligned} \tag{4.58}$$

$$\begin{aligned}
&C_{3311}^{i}\varepsilon_{11}^{0} + C_{3322}^{i}\varepsilon_{22}^{0} + C_{3333}^{i}\varepsilon_{33}^{0} + C_{3311}^{i}S_{1111}\varepsilon_{11}^{0} + C_{3322}^{i}S_{2211}\varepsilon_{11}^{*} + C_{3333}^{i}S_{3311}\varepsilon_{11}^{*} + \\
&C_{3311}^{i}S_{1122}\varepsilon_{11}^{*} + C_{3322}^{i}S_{2222}\varepsilon_{11}^{*} + C_{3333}^{i}S_{3322}\varepsilon_{11}^{*} + C_{3311}^{i}S_{1133}\varepsilon_{11}^{*} + C_{3322}^{i}S_{2233}\varepsilon_{11}^{*} + \\
&C_{3333}^{i}S_{3333}\varepsilon_{11}^{*} = C_{3311}^{m}\varepsilon_{11}^{0} + C_{3322}^{m}\varepsilon_{22}^{0} + C_{3333}^{m}\varepsilon_{33}^{0} + C_{3311}^{m}S_{1111}\varepsilon_{11}^{*} + C_{3322}^{m}S_{2211}\varepsilon_{11}^{*} + \\
&C_{3333}^{m}S_{3311}\varepsilon_{11}^{*} + C_{3311}^{m}S_{1122}\varepsilon_{11}^{*} + C_{3322}^{m}S_{2222}\varepsilon_{11}^{*} + C_{3333}^{m}S_{3322}\varepsilon_{11}^{*} + C_{3311}^{m}S_{1133}\varepsilon_{11}^{*} + \\
&C_{3322}^{m}S_{2233}\varepsilon_{11}^{*} + C_{3333}^{m}S_{3333}\varepsilon_{11}^{*} - C_{3311}^{m}\varepsilon_{11}^{*} - C_{3322}^{m}\varepsilon_{22}^{*} - C_{3333}^{m}\varepsilon_{33}^{*}
\end{aligned} \tag{4.59}$$

In the above three equation the Eshelby's tensor are defined by

$$S_{1111} = \frac{3}{8\pi(1-\nu)}a_1^2 I_{11} + \frac{1-2\nu}{8\pi(1-\nu)}I_1 \tag{4.60}$$

$$S_{2222} = \frac{3}{8\pi(1-\nu)} a_2^2 I_{22} + \frac{1-2\nu}{8\pi(1-\nu)} I_2 \tag{4.61}$$

$$S_{3333} = \frac{3}{8\pi(1-\nu)} a_3^2 I_{33} + \frac{1-2\nu}{8\pi(1-\nu)} I_3 \tag{4.62}$$

$$S_{1122} = \frac{1}{8\pi(1-\nu)} a_2^2 I_{12} - \frac{1-2\nu}{8\pi(1-\nu)} I_1 \tag{4.63}$$

$$S_{1133} = \frac{1}{8\pi(1-\nu)} a_3^2 I_{13} - \frac{1-2\nu}{8\pi(1-\nu)} I_1 \tag{4.64}$$

$$S_{2211} = \frac{1}{8\pi(1-\nu)} a_1^2 I_{21} - \frac{1-2\nu}{8\pi(1-\nu)} I_2 \tag{4.65}$$

$$S_{2233} = \frac{1}{8\pi(1-\nu)} a_3^2 I_{23} - \frac{1-2\nu}{8\pi(1-\nu)} I_2 \tag{4.67}$$

$$S_{3311} = \frac{1}{8\pi(1-\nu)} a_1^2 I_{31} - \frac{1-2\nu}{8\pi(1-\nu)} I_3 \tag{4.68}$$

$$S_{3322} = \frac{1}{8\pi(1-\nu)} a_2^2 I_{32} - \frac{1-2\nu}{8\pi(1-\nu)} I_3 \tag{4.69}$$

Since a_1 is the principle axis and a_2, a_3 are same, elliptical integrals in the 23 direction become equal i.e.

$$\begin{aligned} &I_2 = I_3 \\ &I_{22} = I_{33} \\ &I_{12} = I_{13} = I_{21} = I_{31} \\ &I_{23} = I_{32} \end{aligned} \tag{4.70}$$

The integrals are defined by the following formulae

$$I_2 = I_3 = \frac{2\pi a_1 a_3^2}{(a_1^2 - a_3^2)^{3/2}} \left\{ \frac{a_1}{a_3} \left(\frac{a_1^2}{a_3^2} - 1 \right)^{1/2} - \cos^{-1} h \frac{a_1}{a_3} \right\} \tag{4.71}$$

$$I_{23} = \frac{\pi}{a_2^2} - \frac{(I_2 - I_1)}{4(a_1^2 - a_2^2)} \tag{4.72}$$

$$I_1 = 4\pi - 2I_2$$

$$3I_{22} = \frac{4\pi}{a_2^2} - I_{23} - \frac{(I_2 - I_1)}{(a_1^2 - a_2^2)} \tag{4.73}$$

$$I_{12} = \frac{(I_2 - I_1)}{(a_1^2 - a_2^2)}$$

$$3I_{11} = \frac{4\pi}{a_1^2 - 2I_{12}}$$

Putting $a_1 = 50, a_2 = 25 \,\&\, a_3 = 25$ and $\nu = 0.4$ .The Integrals end up to the following values and they are tabulated below

Table 4.5 I values –Normal component

I_1=2.18107	I_2=5.19265	I_3=5.19265
I_{11}=0.000604	I_{12}=0.001606	I_{13}=0.001606
I_{21}=0.00160618	I_{22}=0.004625	I_{23}=0.004625
I_{31}=0.00160	I_{32}=0.004625	I_{33}=0.004625

Substituting the above tabulated I values into S equation we obtain the S values for different normal components. They are tabulated in the following table

Table 4.6 S values – Normal component.

$S_{1111} = 0.329696$	$S_{2222} = 0.643942$	$S_{3333} = 0.643942$
$S_{1122} = 0.0376432$	$S_{2211} = 0.197413$	$S_{3311} = 0.197413$
$S_{1133} = 0.0376432$	$S_{2233} = 0.122821$	$S_{3322} = 0.122821$

From equation (4.11) for an isotropic material we have

$$C_{ijkl} = \lambda\delta_{ij}\delta_{kl} + \mu\delta_{jk}\delta_{jl} + \mu\delta_{il}\delta_{jk} \tag{4.75}$$

For normal direction the above equation can be written in index notation as

$$C_{1111} = \lambda\delta_{11}\delta_{11} + \mu\delta_{11}\delta_{11} + \mu\delta_{11}\delta_{11} \tag{4.76}$$

Applying Kronecker's delta definition from equation (4.12), we obtain

$$C_{1111} = \lambda\times1\times1 + \mu\times1\times1 + \mu\times1\times1 \tag{4.77}$$

$$C_{1111} = \lambda + 2\mu \tag{4.78}$$

Similarly for 1122 and 1133 components it can written as

$$C_{1122} = \lambda\delta_{11}\delta_{22} + \mu\delta_{12}\delta_{12} + \mu\delta_{12}\delta_{12} \tag{4.79}$$

$$C_{1122} = \lambda\times1\times1 + \mu\times0\times0 + \mu\times0\times0 \tag{4.80}$$

$C_{1122} = \lambda$ And (4.81)

$C_{1133} = \lambda\delta_{11}\delta_{33} + \mu\delta_{13}\delta_{13} + \mu\delta_{13}\delta_{13}$ (4.82)

$C_{1133} = \lambda$ (4.83)

Writing all the terms of elastic modulas for matrix and Inclusion and substituting the values of μ and λ from table 4.1 the following table is tabulated.

Table 4.7 Elastic Modulus of Normal components for Matrix

$C^m_{1111} = 5.093 \times 10^9$	$C^m_{2222} = 5.093 \times 10^9$	$C^m_{3333} = 5.093 \times 10^9$
$C^m_{1122} = 3.633 \times 10^9$	$C^m_{2211} = 3.633 \times 10^9$	$C^m_{3311} = 3.633 \times 10^9$
$C^m_{1133} = 3.633 \times 10^9$	$C^m_{2233} = 3.633 \times 10^9$	$C^m_{3322} = 3.633 \times 10^9$

Table 4.8 Elastic Modulus of Normal components for Inclusion

$C^i_{1111} = 2.83 \times 10^{11}$	$C^i_{2222} = 2.83 \times 10^{11}$	$C^i_{3333} = 2.83 \times 10^{11}$
$C^i_{1122} = 1.2165 \times 10^{11}$	$C^i_{2211} = 1.2165 \times 10^{11}$	$C^i_{3311} = 1.2165 \times 10^{11}$
$C^i_{1133} = 1.2165 \times 10^{11}$	$C^i_{2233} = 1.2165 \times 10^{11}$	$C^i_{3322} = 1.2165 \times 10^{11}$

Substituting all the above elastic modulus values for the matrix and the inclusion from Tables 4.5 and 4.6, and also the S values from Table 4.5 into the three simultaneous equations and solving for the three equations, we obtain

$$\varepsilon_{11}^{*}=1.32157\,\varepsilon_{11}^{0}-0.0031372\;\varepsilon_{22}^{0}-0.46917\,\varepsilon_{33}^{0} \tag{4.84}$$

$$\varepsilon_{22}^{*}=1.21456\,\varepsilon_{11}^{0}+3.17357\;\varepsilon_{22}^{0}+1.14597\,\varepsilon_{33}^{0} \tag{4.85}$$

$$\varepsilon_{33}^{*}=1.21456\,\varepsilon_{11}^{0}+1.21443\,\varepsilon_{22}^{0}+3.19511\,\varepsilon_{33}^{0} \tag{4.86}$$

Using the above equations and putting them back into stress equations, we obtain

$$\sigma_{11} = 2.83\times10^{11}(0.114\varepsilon_{11}^{0} + 0.02102\varepsilon_{22}^{0} - 0.31163\varepsilon_{33}^{0})$$

$$\sigma_{22} = 2.83\times10^{11}(0.4705\varepsilon_{11}^{0} + 1.01116\varepsilon_{22}^{0} + 0.1655\varepsilon_{33}^{0}) \tag{4.87}$$

$$\sigma_{33} = 2.83\times10^{11}(-0.4704\varepsilon_{11}^{0} + 0.0111\varepsilon_{22}^{0} - 1.01113\varepsilon_{33}^{0})$$

The quantities, ε_{11}^{0}, ε_{22}^{0} and ε_{33}^{0}, are obtained by the Ansys simulation problem to numerically evaluate the stress in ellipsoidal inclusion.

4.6.1 Finite Element Model

We will now focus on the finite element modeling of the ellipsoidal problem. The matrix and the ellipsoidal inclusion are modeled using the same method as discussed in Chapter 3, but instead of the shear force on the matrix region, we apply a constant normal force of 100 MPa. Our primary interest is to study the stresses in the normal direction, *i.e.*, along the 11, 22 and 33 components or the XX,YY and ZZ components . The following figure shows the FEM model.

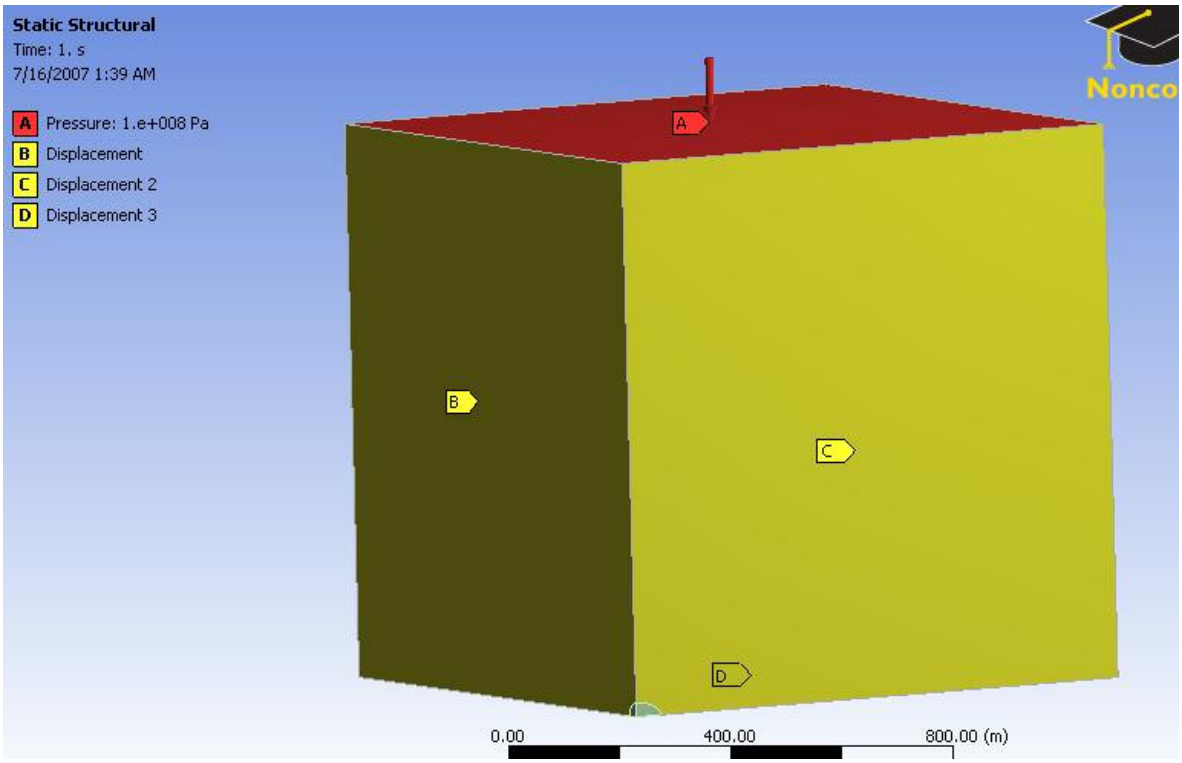

Figure 4.9 FEM model of matrix and inclusion

4.6.2 Ansys Post Processing

For the stress σ_{12}^{0} = 10 M Pa that is applied at infinity on matrix boundary we obtain corresponding normal strains ε_{11}^{0}, ε_{22}^{0} and ε_{33}^{0} strain at infinity, this value is numerically obtained from the strain plot curve in the Ansys simulation post processing result. The following plot shows it.

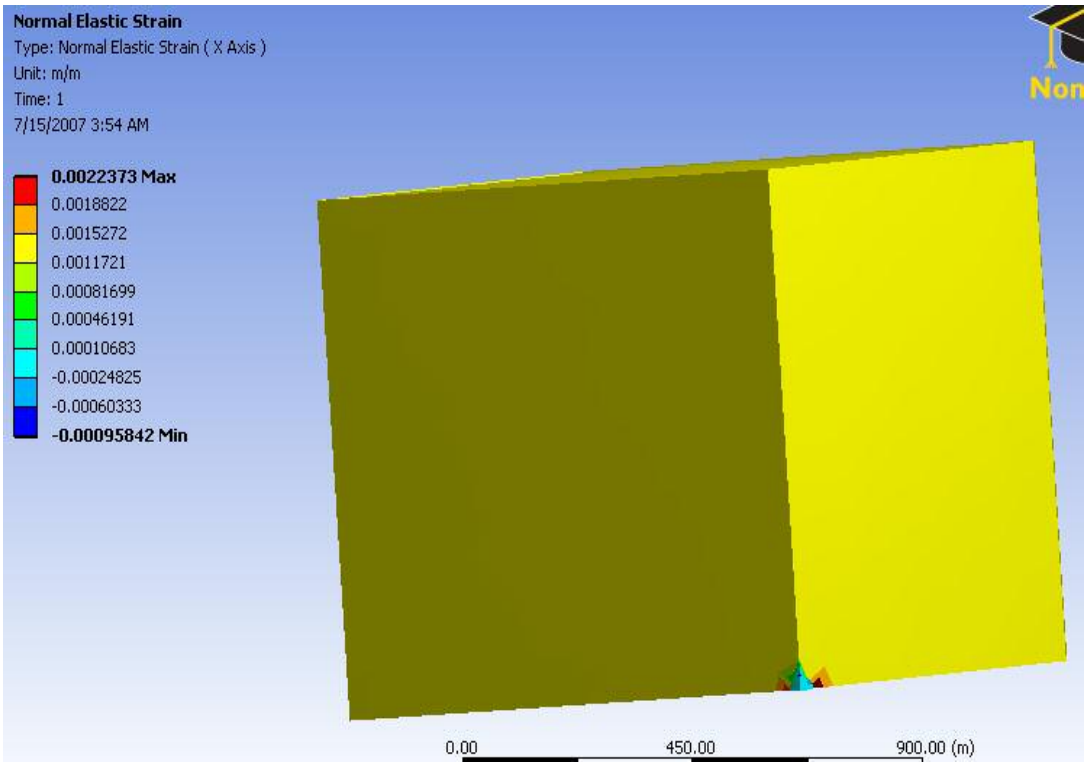

Figure 4.10 The strain plot in 11 direction

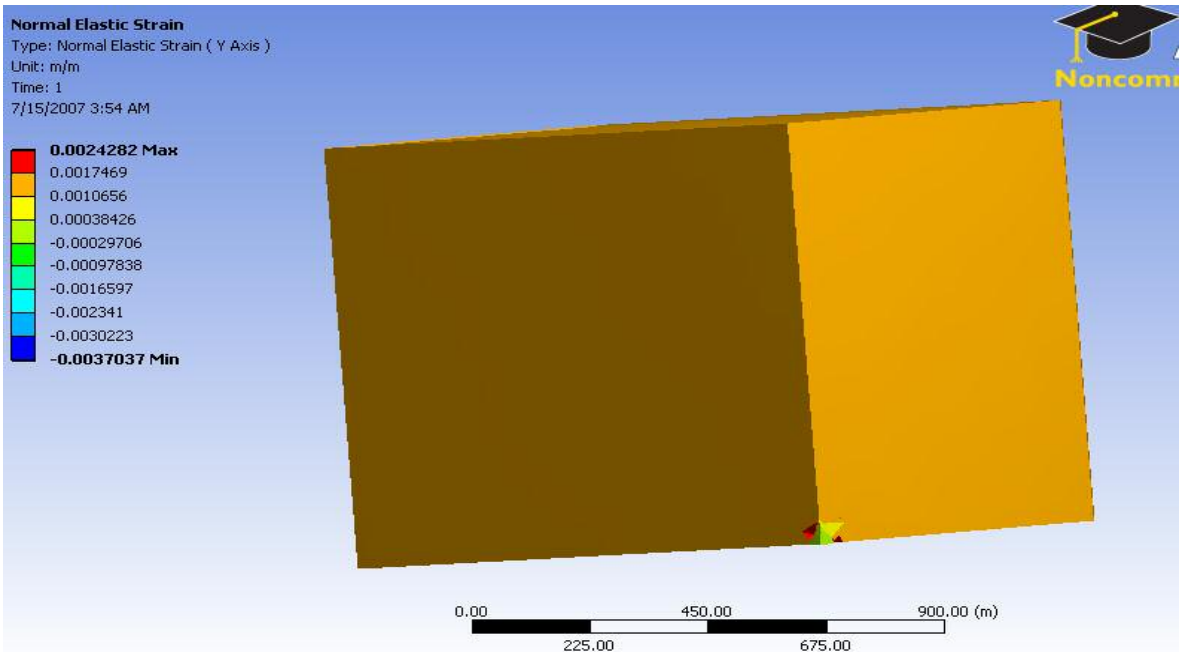

Figure 4.11 The strain plot in 22 direction

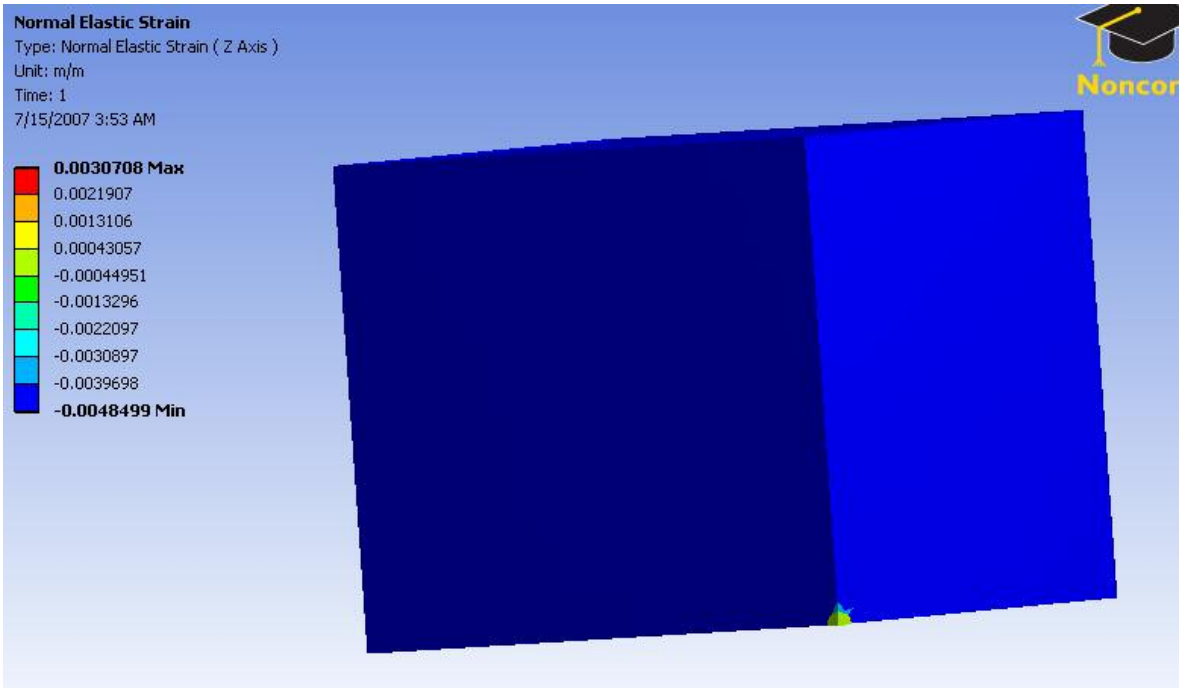

Figure 4.12 The strain plot in 33 direction

From the above plot we can see that ε_{11}^{0}=0.0022373, ε_{22}^{0}= 0.0024282 and ε_{33}^{0}=0.0030708, substituting them into (4.84), (4.85) and (4.86) we obtain theoretical values

$$\sigma_{11} = -0.213 \text{ G Pa} \tag{4.88}$$

$$\sigma_{22} = 1.136 \text{ G Pa} \tag{4.89}$$

$$\sigma_{33} = -1.168 \text{ G Pa} \tag{4.90}$$

The Ansys stress plot in 11, 22 and 33 can be obtained from the following stress plot

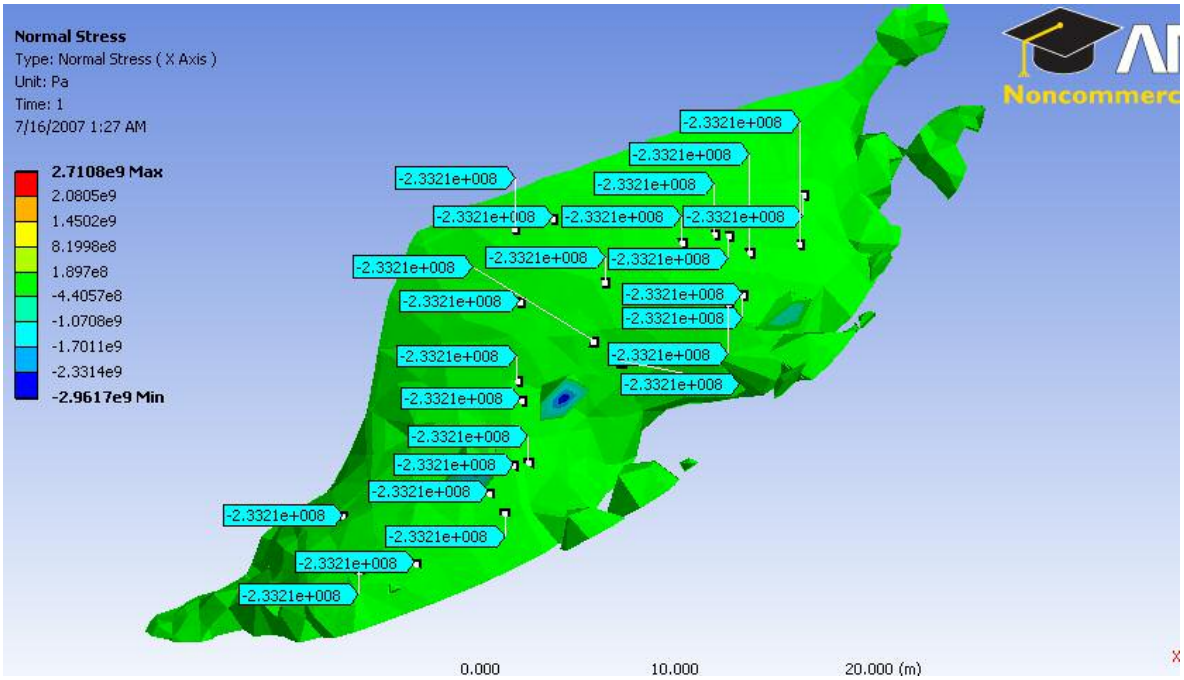

Figure 4.13 The stress plot in 11 direction

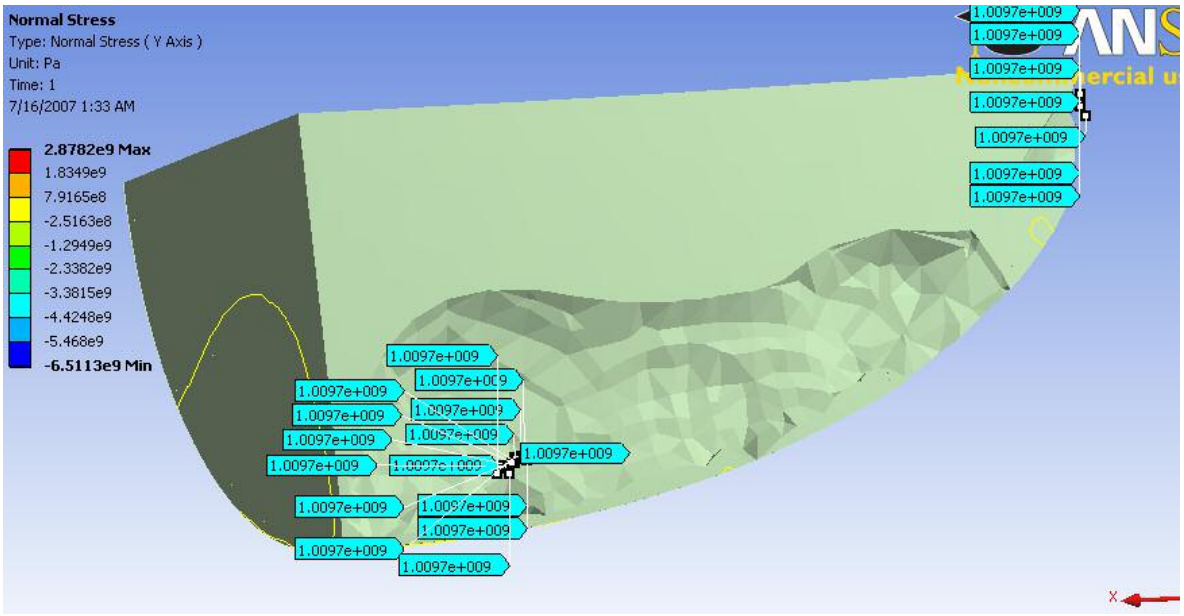

Figure 4.14 strain plot in 33 direction

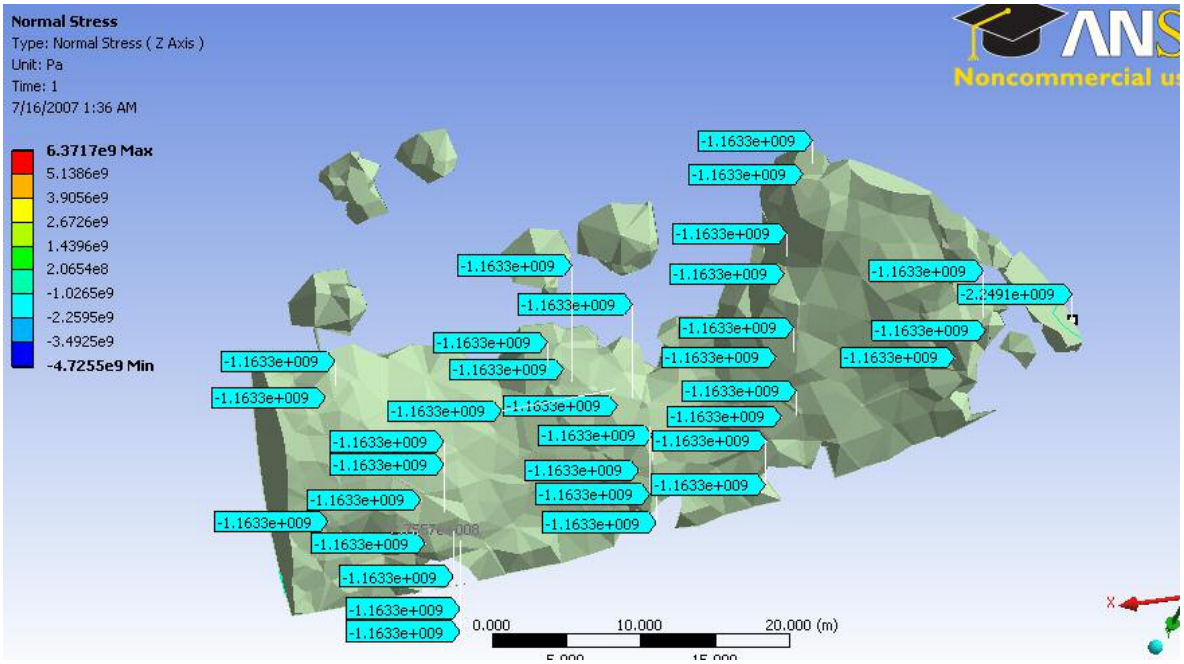

Figure 4.15 The strain plot in 33 directions

Table 4.9 Comparison between the ansys and theoretical values

	Theoretical Value (G Pa)	Ansys (G Pa)
σ_{11}	-0.213	-0.2331
σ_{22}	1.136	1.0097
σ_{33}	-1.168	-1.1633

As we change the aspect ratio of the ellipsoidal inclusion and subject it to the same loading and boundary conditions, *i.e*., if we increase the ratio of a_1 axes to ratio of a_2 axis monotonically from 2, 5 upto 100, we see that the stress inside the ellipsoidal inclusion increases with the aspect ratio and then becomes constant when the ellipsoid shape approximates itself to a cylinder. The following table gives the S values, strain values and stress values obtained for different aspect ratios of the ellipsoidal inclusion.

Table-4.10 Stress, Strain and S values (Normal components)

Aspect Ratio $\left(\frac{a_1}{a_2}\right)$	S	Strain $(\varepsilon_{11}^0, \varepsilon_{22}^0 \& \varepsilon_{33}^0)$	Stress(theory) $(\sigma_{11}^0, \sigma_{22}^0 \& \sigma_{33}^0)$,G Pa	Stress(ansys) $(\sigma_{11}^0, \sigma_{22}^0 \& \sigma_{33}^0)$,G Pa
2	S_{1111}=0.329696 S_{2222}=0.643942 S_{3333}=0.643942	ε_{11}^0=0.0022373 ε_{22}^0=0.0024282 ε_{33}^0=0.0030708	σ_{11}^0= -0.2132 σ_{22}^0=1.136 σ_{33}^0=-1.168	σ_{11}^0= -0.2332 σ_{22}^0= 1.0097 σ_{33}^0=-1.1633
5	S_{1111}=0.119948 S_{2222}=0.692841 S_{3333}=0.692841	ε_{11}^0=0.029283 ε_{22}^0=0.032369 ε_{33}^0=0.0045505	σ_{11}^0=-4.37 σ_{22}^0=5.45 σ_{33}^0=-7.864	σ_{11}^0=-4.12 σ_{22}^0=5.12 σ_{33}^0=-7.13
10	S_{1111}=0.0461904 S_{2222}=0.703678 S_{3333}=0.703678	ε_{11}^0=0.059926 ε_{22}^0=0.04269 ε_{33}^0=0.005265	σ_{11}^0=-8.62 σ_{22}^0=10.69 σ_{33}^0=-13.962	σ_{11}^0=-9.01 σ_{22}^0=10.20 σ_{33}^0=-13.97

Table4.9-Continued

20	S_{1111}=0.0159512 S_{2222}=0.707004 S_{3333}=0.707004	ε_{11}^{0}=0.06776 ε_{22}^{0}=0.05297 ε_{33}^{0}=0.006265	σ_{11}^{0}=-13.72 σ_{22}^{0}=12.61 σ_{33}^{0}=-17.186	σ_{11}^{0}=-13.43 σ_{22}^{0}=12.66 σ_{33}^{0}=-17.913
50	S_{1111}=0.0035159 S_{2222}=0.708089 S_{3333}=0.708089	ε_{11}^{0}=0.07176 ε_{22}^{0}=0.05347 ε_{33}^{0}=0.006916	σ_{11}^{0}=-15.671 σ_{22}^{0}=13.713 σ_{33}^{0}=-25.179	σ_{11}^{0}=-15.123 σ_{22}^{0}=13.861 σ_{33}^{0}=-25.749
100	S_{1111}=0.00106316 S_{2222}=0.708266 S_{3333}=0.708266	ε_{11}^{0}=0.08169 ε_{22}^{0}=0.06179 ε_{33}^{0}=0.007192	σ_{11}^{0}=-15.977 σ_{22}^{0}=13.979 σ_{33}^{0}=-25.820	σ_{11}^{0}=-15.331 σ_{22}^{0}=13.867 σ_{33}^{0}=-25.120

CHAPTER 5

CONCLUSION AND FUTURE SCOPE OF WORK

5.1Conclusion

In this thesis the mathematical model of the ellipsoidal inclusion was done based on equivalent inclusion principle. And also the Finite Element Modeling of the matrix-inclusion pair was done and stress distribution in the matrix-and more importantly in the inclusion region was analyzed. The interface contact between the ellipsoid and the matrix was modeled using bonded contact element. The numerical results obtained was agreeable with the theoretical result .And the stress and strain values inside the ellipsoidal inclusion was uniform as predicted by J D Eshelby's hypothesis [1] .The analysis was also done for varying aspect ratios of the inclusion and varying the elastic modulus of inclusion., keeping constant matrix properties. The stress values obtained were varying monotonically with respect the each other and became constant after they the ellipsoid shape nears to the shape of a cylinder. This study can be extended for particulate composite materials.

5.2 Future Scope of Work

1. We studied the stress analysis for a spherical and prolate shaped ellipsoid shaped inclusion but inclusions come in various shapes like penny, oblate, disc and elliptical cylinder. So we can extend the work all the other inclusion shapes.

2. This work can be also extended to multiple inclusion matrix models.

3. In addition of stress analysis for isotropic materials it can also be extended to non- isotropic materials.

4. We also can try to calculate the elastic strain energy of the inclusion region.

REFERENCES

[1] J D Eshelby- The Determination of the Elastic Field of an Ellipsoidal Inclusion, and Related Problems *Proceedings of the Royal Society of London. Series A, Mathematical and Physical Sciences*, Vol. 241, No. 1226. (Aug. 20, 1957), pp. 376-396

[2] J D Eshelby- The Force on an Elastic Singularity *Philosophical Transactions of the Royal Society of London. Series A, Mathematical and Physical Sciences*, Vol. 244, No. 877 . (Nov. 6, 1951), pp . 87-112.

[3] A model for composites containing three-dimensional ellipsoidal inclusionsK.Y. Lee, D.R. Paul

[4] Micromechanics of Defects in Solids, Toshio Mura

[5] Fundamentals of Defects and Fracture, B. A. Bilby, K J Miller and J. R. Wills

[6] Generalization of Eshelby's Formula for a Single Ellipsoidal Elastic Inclusion to Poroelasticity and Thermoelasticity James G. Berryman *Lawrence Livermore National Laboratory, P.O. Box 808 L-202, Livermore, California 94551-9900*

[7] Elastic Inclusions and Inhomogeneities in Transversely Isotropic Solids H. Y. Yu; S. C. Sanday; C. I. Chang *Proceedings: Mathematical and Physical Sciences*, Vol. 444, No. 1920.(Jan. 8, 1994), pp.239-252.

[8] Ansys Workbench Tutorial by Kent Lawence

[9] Mathematica Tutorial 5

[10] On the Eshelby's Inclusion Problem for Ellipsoids with Nonuniform Dilatational Gaussian and Exponential Eigen strains P Sharma and R Sharma

BIOGRAPHICAL INFORMATION

Mahesh Kailas received his Bachelor of Engineering degree form Visveswaraiah Technological University, India, in 2002. He received his M.S. degree in Mechanical Engineering from The University of Texas at Arlington in 2007. His research interests are in the field of design, nanostructures and finite element analysis. His thesis master's thesis involved finite element modeling of ellipsoidal inclusion...